

Cyclotriphosphazenes as Scaffolds for the Synthesis of Metallomesogens

Josefina Jiménez,* José Antonio Sanz, José Luis Serrano, Joaquín Barberá, and Luis Oriol

Cite This: <https://dx.doi.org/10.1021/acs.inorgchem.0c00124>

Read Online

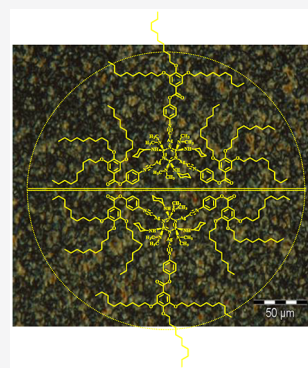
ACCESS |

Metrics & More

Article Recommendations

Supporting Information

ABSTRACT: (Amino)cyclotriphosphazenes have been used as new scaffolds for the synthesis of silver(I) metallomesogens. Two cyclotriphosphazenes, $[N_3P_3(NHCy)_6]$ (**phos-1**) and *nongem-trans*- $[N_3P_3(NHCy)_3(NMe_2)_3]$ (**phos-2**), were reacted with the silver complex having a promesogenic ligand, $[Ag(OTf)L]$ ($L = CNC_6H_4\{OC(O)C_6H_2(3,4,5-(OC_{10}H_{21})_3)\}_4$; $OTf = OSO_2CF_3$), in different molar ratios, 1:1, 1:2, or 1:3, to give two series of cationic metallophosphazenes, $[N_3P_3(NHCy)_6\{AgL\}_n](TfO)_n$ (**phos-1.n**) and *nongem-trans*- $[N_3P_3(NHCy)_3(NMe_2)_3\{AgL\}_n](TfO)_n$ (**phos-2.n**) with $n = 1, 2, \text{ or } 3$. The chemical structure of these compounds, deduced from spectroscopic techniques, was in accordance with coordination of the silver fragments “AgL” to nitrogen atoms of the phosphazene ring, whereby their number n depends on the molar ratio used. Despite the presence of the bulky substituents on the core N atoms, cyclotriphosphazenes coordinated to three “AgL” units exhibited mesomorphism at room temperature. The mesophase was characterized as columnar hexagonal according to the optical microscopy and X-ray diffraction studies. A model based on an intermolecular association in pairs of the metallo-cyclotriphosphazenes having three AgL units has been proposed in order to explain the mesomorphic columnar arrangement in these materials. Starting silver complex, $[Ag(OTf)L]$, also exhibited a columnar hexagonal mesophase at room temperature.



1. INTRODUCTION

Metal-containing liquid crystals, also known as metallomesogens, can expand the properties of conventional liquid crystals usually based on totally organic materials.¹ The presence of metal atoms opens up the possibility of new structures in the design of liquid crystals derived from the metal geometries of organometallic and coordination compounds. Besides, metal entities modify the physical properties of conventional liquid crystals based on organic materials, such as magnetic, electric, or optical properties. A large variety of complexes have been described as mesomorphic so far using different metal entities. Silver(I) derivatives are of particular interest in the field of liquid crystals due to ability to yield ionic liquid crystals and their structural motifs compatible with the mesomorphism.² Stilbazole derivatives have been most widely used ligands for the preparation of both calamitic and columnar Ag(I) mesomorphic materials^{3a} from the pioneering work by Bruce and co-workers.^{3b} Although to far less an extent, isocyanides have been also described as versatile ligands for the preparation of mesogenic ionic Ag(I) complexes either having calamitic or columnar mesomorphism depending on the number of peripheral aliphatic chains of the ligands.⁴ The mesomorphic arrangement of functional ligands connected with the particular properties introduced by silver atoms has recently been applied to the preparation of ion-conductive functional materials⁵ or organic semiconductors, among other applications.⁶ Nevertheless, the silver(I) liquid crystalline complexes described so far have a conventional structure. Cyclo-

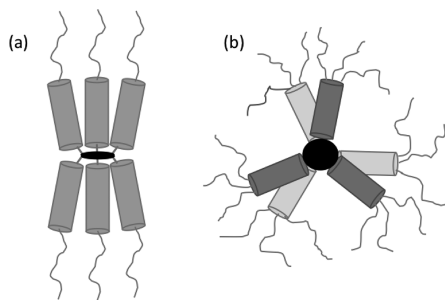
triphosphazenes provide new possibilities to the design of metallomesogens by using as a core with three nitrogen atoms able to coordinate metallic entities, e.g., silver(I) derivatives, and with additional substitution on the P atoms.

Phosphazenes, $[NPR_2]$, are an important type of inorganic compounds, whose properties can be tailored by the choice of appropriate side groups on phosphorus, R.⁷ They are usually prepared by nucleophilic substitution reactions that involve the use of halophosphazene, $[NPCl_2]$, cyclic trimers, or high polymers as substrates for reactions with alkoxides, aryloxides, or amines.^{7,8} In addition, with few restrictions, organic side groups incorporated into a phosphazene can themselves be modified by exposure to reagents that introduce additional functionality,⁹ as has been recently reviewed.¹⁰ Thus, trimers or polymers with all the chloro atoms replaced by promesogenic units have been prepared in an effort to obtain liquid crystalline materials.¹¹ Specifically, cyclotriphosphazenes have proved to be useful as a multiarmed central core upon which mesogenic units have been linked to the phosphorus atoms to give supermolecular liquid crystals.¹² In this regard,

Received: January 13, 2020

we have reported several series of these nonconventional liquid crystals with the pro-mesogenic units directly attached to the ring phosphorus atoms,¹³ whose mesomorphic properties strongly depend on a suitable volume balance between the rigid core and the alkyl chains in the pro-mesogenic group ranging from calamitic to discotic and to cubic mesomorphism when the number of terminal alkyl chains increases. Calamitic mesomorphism is promoted by monosubstituted units (e.g., having one terminal alkyl chain or monocatenar), and this behavior was explained in terms of the model shown in Chart 1a.^{13a,b,14} Columnar or cubic phases resulted from the

Chart 1. Schematic Models for Calamitic Structure of Cyclophosphazenes and Star-Shaped Structure of Cyclophosphazenes with Polycatenar Moieties^a



^a(a) Calamitic structure of cyclophosphazenes with monocatenar moieties, which point upwards and downwards regarding the cyclophosphazene ring; (b) the star-shaped structure of cyclophosphazenes with polycatenar moieties, which arrange themselves parallel to the cyclophosphazene ring (represented as a black circle) in two levels (mesogens in the upper level indicated with a darker color and in lower level with a lighter color).

incorporation of polycatenar units, which promote from a hexagonal columnar mesophase to a cubic mesophase upon increasing the number of chains in the periphery of the system. The columnar mesomorphism was explained in terms of the model shown in Chart 1b.¹³

Phosphazenes, trimers, or polymers, can also be used as scaffolds for the design and construction of a variety of ligands,^{15,16} to coordinate to metals. The facile substitution of P–Cl bonds in cyclic trimer or polymer allows ready construction of phosphazenes carrying additional peripheral donor functions giving a library of multisite coordination ligands. Indeed, the backbone nitrogen atoms have sufficient basicity to coordinate to metals depending on the electronic properties of the exocyclic substituents at phosphorus. Alkyl, aryl, and primary and secondary organo amino substituents enhance the donor ability of backbone N atoms.^{16c} Silver derivatives of phosphazenes (cyclic or polymers) are also

known, both with the metal coordinated to peripheral donor atoms¹⁷ and coordinated to the backbone N atoms.¹⁸ We have also contributed to this field by reporting metalocyclo- and polyphosphazenes containing gold or silver coordinated to exocyclic 4-oxypyridine groups and their thermolytic transformation into nanostructured materials or into metallic micro- and nanostructures deposited on silicon and silica surfaces.¹⁹ We have also recently explored the reactivity of the multisite (amino)cyclotriphosphazene ligands with the silver complexes [Ag(OTf)L] (L = PPh₃ or PPh₂Me; OTf = OSO₂CF₃) and obtained two series of the cationic metallophosphazenes, [N₃P₃(NHCy)₆{AgL}_n](TfO)_n and *nongem-trans*-[N₃P₃(NHCy)₃(NMe₂)₃{AgL}_n](TfO)_n (*n* = 2 or 3, L = PPh₃ or PPh₂Me), in which the silver moieties “AgL” are coordinated to the nitrogen atoms of the phosphazene ring (see Chart 2) and which have outstanding biological properties.²⁰ However, to the best of our knowledge, there are no reports of metallophosphazenes with liquid crystalline properties.

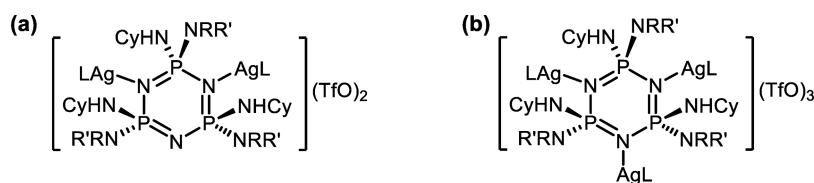
Herein, the reactivity of (amino)cyclotriphosphazene ligands has been explored in order to obtain new silver(I) metal-omesogens. Two cyclotriphosphazenes were used, a single-substituent trimer having six cyclohexylamine units linked to the P atoms, [N₃P₃(NHCy)₆] (**phos-1**), and a mixed-substituent trimer having three cyclohexylamino and three dimethylamino units linked to the P atoms in a *nongeminal-trans* arrangement (i.e., 2,4,6-*trans*-[N₃P₃(NHCy)₃(NMe₂)₃] (**phos-2**); see Chart 3a). A strategy similar to the one used to obtain derivatives shown in Chart 2 was performed but this time with a starting silver complex having a pro-mesogenic ligand, [Ag(OTf)L] (L = CNC₆H₄{OC(O)C₆H₂(3,4,5-(OC₁₀H₂₁)₃)}-4; OTf = OSO₂CF₃) (see Chart 3b) instead of a phosphane ligand. Thus, two series of cationic metallophosphazenes have been obtained, [N₃P₃(NHCy)₆{AgL}_n](TfO)_n (**phos-1.n**) and *nongem-trans*-[N₃P₃(NHCy)₃(NMe₂)₃{AgL}_n](TfO)_n (**phos-2.n**) with *n* = 1, 2, or 3, in which the silver fragments “AgL” are coordinated to nitrogen atoms of the phosphazene ring. The thermal and mesomorphic properties of this new series of cyclophosphazenes are also reported here in an effort to continue the exploration of these nonconventional structures.

2. RESULTS AND DISCUSSION

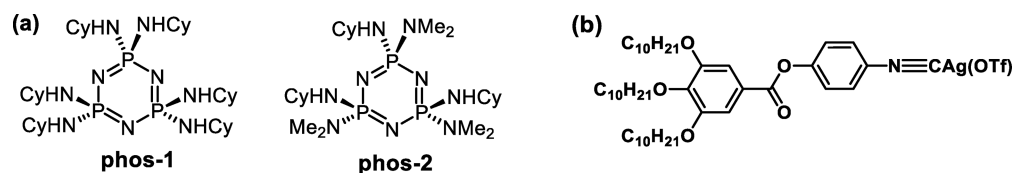
2.1. Synthesis and Characterization of the Metallophosphazenes. The isocyanide ligand and the starting silver complex, [Ag(OTf)L], used in this work, were prepared according to literature methods,^{4b,21,22} as shown in Scheme 1; see the Experimental Section for details of [Ag(OTf)L].

The synthesis of metallophosphazenes was approached by complexation of the donor nitrogen atoms of an (amino)-cyclophosphazene ring. The reaction of **phos-1** or **phos-2** with

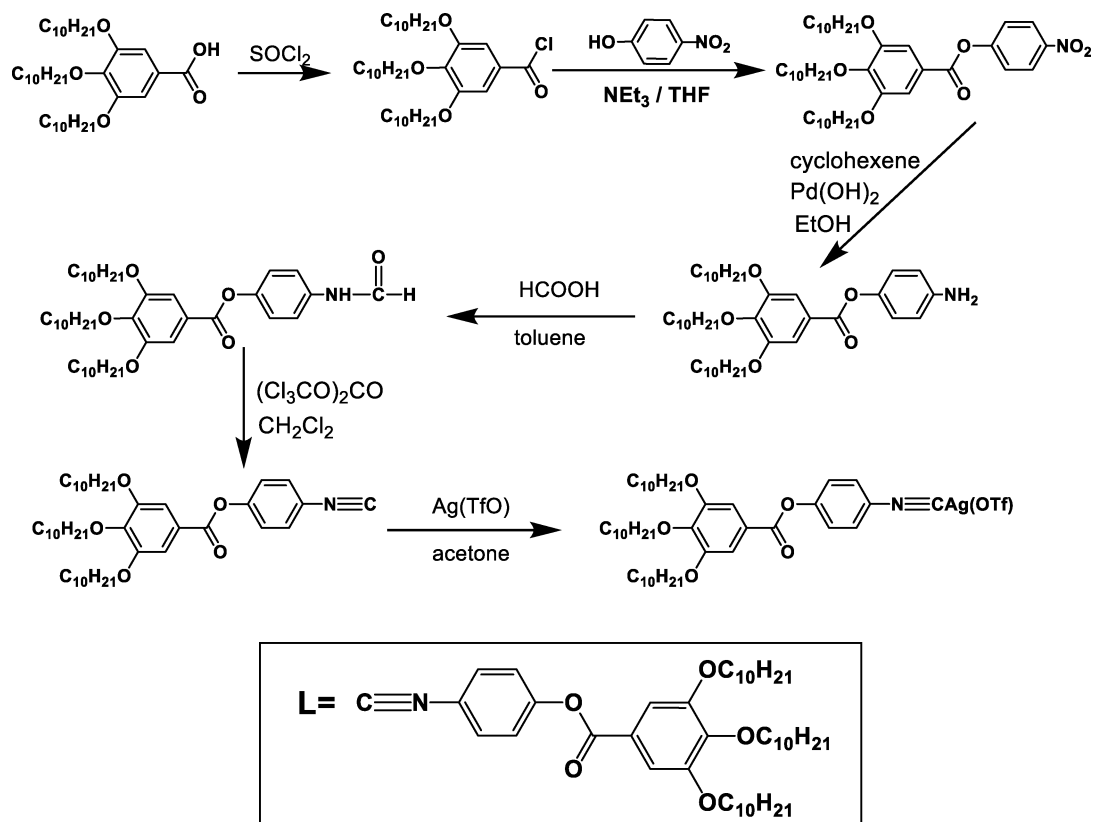
Chart 2. Compounds Obtained in the Reaction of [N₃P₃(NHCy)₃(NRR')₃] (NRR' = NHCy or NMe₂) with [Ag(OTf)L] (L = PPh₃ or PPh₂Me) in a Molar Ratio (a) 1:2 (b) 1:3



NRR' = NHCy or NMe₂; L = PPh₃ or PPh₂Me

Chart 3. Compounds Used in This Work^a

^a(a) (Amino)cyclotriphosphazene trimers used as ligands in this work and (b) starting silver complex used in this work, $[\text{Ag}(\text{OTf})\text{L}]$.

Scheme 1. Synthesis of the Isocyanide Ligand and the Starting Silver Complex, $[\text{Ag}(\text{OTf})\text{L}]$ 

Scheme 2. Synthesis of the New Metallophosphazenes

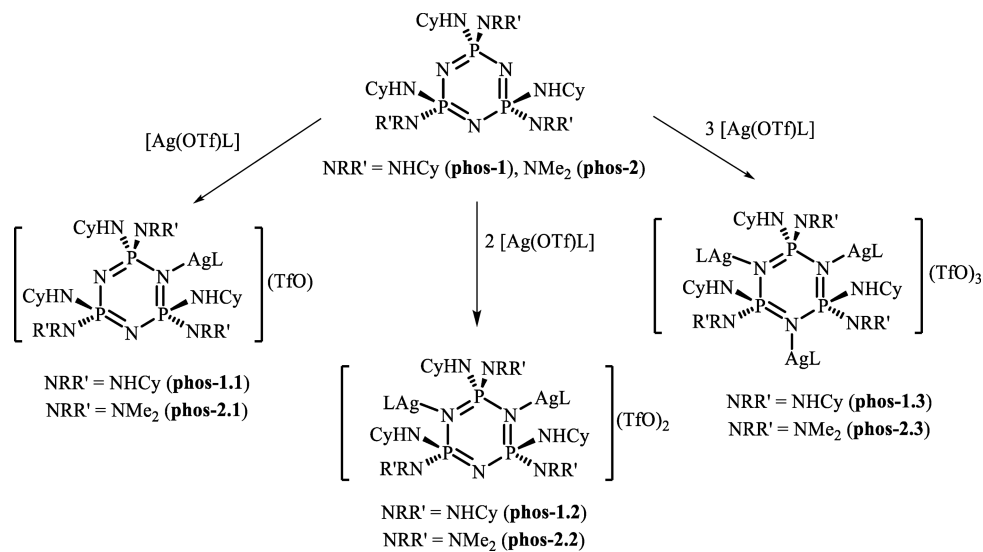


Table 1. $^{31}\text{P}\{^1\text{H}\}$ NMR Spectroscopic Data for Silver Complexes with phos-1 at Room Temperature and at -80°C^a

compound	spin system	T , solvent	$\delta[\text{N}-\text{P}-\text{N}]^b$	$\delta[\text{N}-\text{P}-\text{NAg}]^b$ [$^2J_{\text{P}-\text{P}}]^c$	$\delta[\text{AgN}-\text{P}-\text{NAg}]^b$ [$^2J_{\text{P}-\text{P}}]^c$
phos-1	A_3	RT, CDCl_3^d	14.44 (s)		
phos-1.1	AB_2	RT, CD_2Cl_2		15.19 (s, br)	
		-80°C , CD_2Cl_2	14.09 ("t")	15.98 ("d") [48.2]	
phos-1.2	AB_2	RT, CDCl_3^d			16.71 (s, br)
		-80°C , CD_2Cl_2		13.58 ("d")	17.18 ("t") [35.6]
$[\text{N}_3\text{P}_3(\text{NHCy})_6\{\text{AgPPh}_3\}_2](\text{TfO})_2^e$	AB_2	RT, CDCl_3			16.90 (s, br)
		-80°C , $(\text{CD}_3)_2\text{CO}$		13.23("d")	17.54("t") [36.3]
phos-1.3	A_3	RT, CDCl_3^d			18.97 (s)
		-80°C , CD_2Cl_2			18.35 (s)
$[\text{N}_3\text{P}_3(\text{NHCy})_6\{\text{AgPPh}_3\}_3](\text{TfO})_3^e$	A_3	RT, CDCl_3			18.38 (s)

^aCompounds $[\text{N}_3\text{P}_3(\text{NHCy})_6\{\text{AgPPh}_3\}_n](\text{TfO})_n$ ($n = 2$ or 3) have been included for comparison.²⁰ ^bValues in ppm. ^cValues in Hz. ^dThe data in CD_2Cl_2 at RT, which are given in the Experimental Section, are very similar to those in CDCl_3 . ^eSee ref 20. $[\text{N}_3\text{P}_3(\text{NHCy})_6\{\text{AgPPh}_3\}](\text{TfO})$ with only a silver fragment, "AgPPh₃", is not known. The reaction of $[\text{N}_3\text{P}_3(\text{NHCy})_6]$ with $[\text{Ag}(\text{OTf})\text{PPh}_3]$ in molar ratio 1:1 evolved with the loss of the ligand, PPh₃, and formation of $[\text{N}_3\text{P}_3(\text{NHCy})_6\text{Ag}(\text{TfO})]_n$. That is why we have been unable to compare the signal of phos-1.1 with other similar compounds.

the silver complex $[\text{Ag}(\text{OTf})\text{L}]$ ($\text{L} = \text{CNC}_6\text{H}_4\{\text{OC}(\text{O})\text{C}_6\text{H}_2(3,4,5\text{-}(\text{OC}_{10}\text{H}_{21})_3)\}_4$; $\text{OTf} = \text{OSO}_2\text{CF}_3$), in dichloromethane and in different molar ratios, 1:1, 1:2, or 1:3, led to two series of cationic metallophosphazenes, $[\text{N}_3\text{P}_3(\text{NHCy})_6\{\text{AgL}\}_n](\text{TfO})_n$ (**phos-1.n**) and *nongem-trans*- $[\text{N}_3\text{P}_3(\text{NHCy})_3(\text{NMe}_2)_3\{\text{AgL}\}_n](\text{TfO})_n$ (**phos-2.n**). In all metallophosphazenes obtained, the silver fragments "AgL" are coordinated to nitrogen atoms of the phosphazene ring, whereby their number n depends on the molar ratio used (see Scheme 2).

All the metallophosphazenes were obtained in high yield and are soluble in organic solvents such as dichloromethane, chloroform, or hexane and only slightly soluble in acetone or ethanol. All these compounds and the starting product itself, $[\text{Ag}(\text{OTf})\text{L}]$, were characterized by elemental analysis, IR, ^1H , $^{13}\text{C}\{^1\text{H}\}$, and $^{31}\text{P}\{^1\text{H}\}$ NMR spectroscopy, and MALDI-TOF mass spectrometry. The characterization data are given in the Experimental Section and are consistent with the formulas and structure indicated and, specifically, with the coordination of metals to the backbone nitrogen atoms, as will be mentioned later in detail. All data have been compared with those observed for the similar complexes $[\text{N}_3\text{P}_3(\text{NHCy})_6\{\text{AgL}\}_n](\text{TfO})_n$ or *nongem-trans*- $[\text{N}_3\text{P}_3(\text{NHCy})_3(\text{NMe}_2)_3\{\text{AgL}\}_n](\text{TfO})_n$ ($n = 2$ or 3 ; $\text{L} = \text{PPh}_3$ or PPh_2Me) mentioned before, which were characterized by single-crystal X-ray diffraction, thereby allowing key bonding information to be obtained and in which metals are coordinated to the ring nitrogen atoms.²⁰ IR spectra clearly evidence the coordination of the metal fragments "AgL" to **phos-1** or **phos-2**, showing absorptions attributable to trifluoromethanesulfonate (triflate) units and to the isocyanide ligand, which are all shifted from those in the starting complex $[\text{Ag}(\text{OTf})\text{L}]$. The triflate peaks, which could in principle be used to distinguish covalent and ionic trifluoromethanesulfonate,²³ are not very useful because an unambiguous assignment is hindered by the overlap of CF_3 , SO_3 , and isocyanide vibrational modes.^{19a,22} However, all complexes have very similar bands in shape and position in the stretching region of the triflate ($1280\text{--}1000\text{ cm}^{-1}$, $\nu[\text{SO}_3(\text{E})]$, $\nu[\text{SO}_3(\text{A}_1)]$, $\nu[\text{CF}_3(\text{A}_1)]$, and $\nu[\text{CF}_3(\text{E})]$) (see the Experimental Section). These bands are also similar to those observed for the complexes $[\text{N}_3\text{P}_3(\text{NHCy})_6\{\text{AgL}\}_n](\text{TfO})_n$ or *nongem-trans*- $[\text{N}_3\text{P}_3(\text{NHCy})_3(\text{NMe}_2)_3\{\text{AgL}\}_n](\text{TfO})_n$ ($n = 2$ or 3 ; $\text{L} = \text{PPh}_3$ or PPh_2Me) mentioned before, for which the

presence of ionic trifluoromethanesulfonate was clearly confirmed by single-crystal X-ray structural analyses.²⁰ In addition, the conductivity of **phos-1.1** and **phos-2.1** was measured in dichloromethane. The molar conductivity values (Λ_M) of both compounds were 12 and 15 $\text{ohm}^{-1}\text{ cm}^2\text{ mol}^{-1}$, respectively, which are similar to those of silver 1:1 electrolytes in literature.²² A single peak at approximately -78 ppm appears in the ^{19}F NMR spectra for all synthesized metallophosphazenes. The bands of the characteristic phosphazene absorptions in the IR spectra, such as $\text{P}=\text{N}$ and $\text{C}-\text{N}$ (at 1186 and 1177 cm^{-1} in **phos-1** and at 1180 , 1171 , and 1140 cm^{-1} in **phos-2**), change after coordination of the metal, as also previously observed in other poly- or cyclophosphazenes with silver coordinated to the core nitrogen atoms.^{18c,20} However, new bands corresponding to these peak frequencies could not be assigned in the new metallophosphazenes because of the overlap with CF_3 , SO_3 , and isocyanide vibrational modes. The bands in the $3000\text{--}3400\text{ cm}^{-1}$ region, which are assigned to the $\text{N}-\text{H}$ stretching, are also different from those of the starting phosphazenes. On complexation, only one band at approximately 3300 cm^{-1} is observed for all complexes, which can be attributed to the disruption of the hydrogen bonding of $\text{N}-\text{H}$ groups.^{18c} The IR spectra also show the $\nu(\text{CO})$ and $\nu(\text{CN})$ absorptions from the isocyanide ligand. $\nu(\text{CN})$ absorptions appear at higher wavenumbers (ca. 60 cm^{-1}) than in the free isocyanide, as observed in other isocyanide silver complexes^{4b,21a} and in the starting product itself, $[\text{Ag}(\text{OTf})\text{L}]$. This shift is due to two factors, the σ -donation of the antibonding carbon lone pair to metal and the π -backbonding from metal d orbital to the π^* ligand orbitals.²¹ Besides, in our series of compounds, **phos-1.n** and **phos-2.n** (especially in **phos-1.n**) this $\nu(\text{CN})$ absorption shifts slightly to higher wavenumbers with the rise in the number of silver atoms, which indicates a rise of the σ -donation from isocyanide ligands as a consequence of a lower σ -donation from the phosphazene as the silver atoms increase.

The $^{31}\text{P}\{^1\text{H}\}$ and ^1H NMR spectra in solution are also consistent with the coordination of the metal fragments to the ring nitrogen atoms. The signals observed for complexes with single-substituent trimer **phos-1** in their $^{31}\text{P}\{^1\text{H}\}$ NMR spectra at room temperature (RT) are collected in Table 1. A single peak, shifted downfield from the peak of parent phosphazene, is shown by the phosphazene phosphorus atoms in all

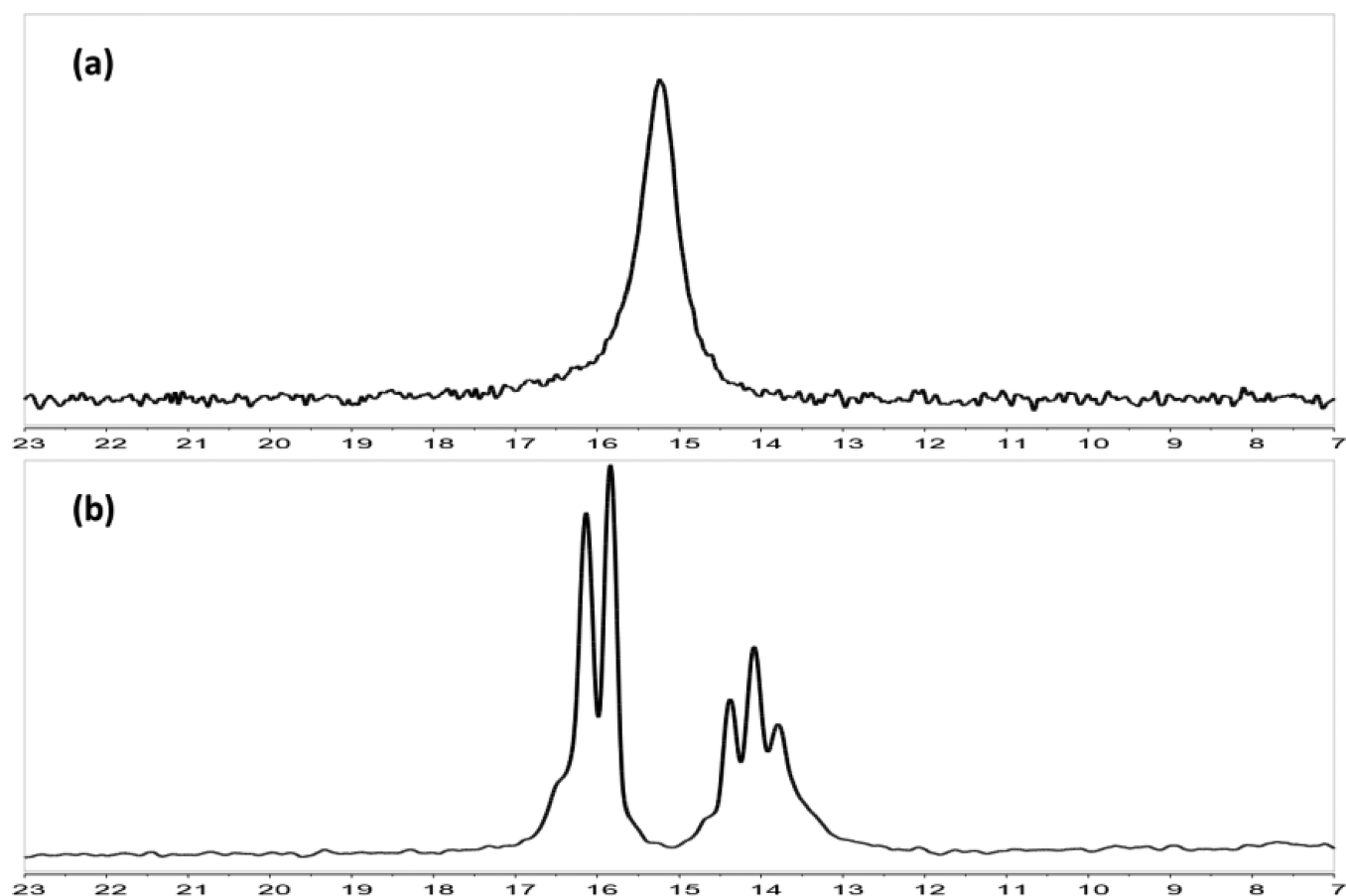


Figure 1. $^{31}\text{P}\{^1\text{H}\}$ NMR spectra of compound **phos-1.1** in CD_2Cl_2 at RT and (b) at -80°C .

Table 2. ^1H NMR Spectroscopic Data for Silver Complexes with **phos-1** at Room Temperature^a

compound	$\delta(\text{CNC}_6\text{H}_4\text{O})$	$\delta(\text{C}_6\text{H}_2)$	$\delta(\text{OCH}_2)$	$\delta(\text{NH})$	$\delta(\text{N}-\text{CH})$	$\delta(\text{CH}_2)$	$\delta(\text{CH}_3)$
L^b	7.45 ("d", 8.9 Hz, 2H); 7.24 ("d", 8.9 Hz, 2H)	7.37 (s, 2H)	4.06 ("t", 6.6 Hz, 2H); 4.03 ("t", 6.6 Hz, 4H)			1.86–1.20 (m, 48 H)	0.88 (m, 9H)
$[\text{Ag}(\text{OTf})\text{L}]$	7.63 ("d", 8.9 Hz, 2H); 7.36 ("d", 8.9 Hz, 2H)	7.37 (s, 2H)	4.07 ("t", 6.4 Hz, 4H); 4.04 ("t", 6.6 Hz, 2H)			1.86–1.23 (m, 48 H)	0.88 (m, 9H)
phos-1				2.0 (br, 6H)	3.05 (m, 6H)	1.94, 1.65, 1.50, 1.26, 1.10 (m, 60 H)	
phos-1.1	7.63 ("d", 8.8 Hz, 2H); 7.34 ("d", 8.8 Hz, 2H)	7.38 (s, 2H)	4.03 (m, 6H)	2.45 (br, 6H)	3.00 (m, 6H)	1.95–1.14 (m, 108H)	0.88 (m, 9H)
phos-1.2	7.71 ("d", 8.8 Hz, 4H); 7.34 ("d", 8.8 Hz, 4H)	7.37 (s, 4H)	4.07 ("t", 6.6 Hz, 4H); 4.04 ("t", 6.6 Hz, 8H)	3.24 (br, 6H)	3.06 (br, 6H)	1.96–1.13 (m, 156H)	0.88 (m, 18H)
phos-1.3	7.71 ("d", 8.8 Hz, 6H); 7.35 ("d", 8.8 Hz, 6H)	7.37 (s, 6H)	4.07 ("t", 6.4 Hz, 6H); 4.04 ("t", 6.4 Hz, 12H)	3.95 (br, 6H)	3.08 (br, 6H)	2.08–1.1 (m, 204H)	0.88 (m, 27H)

^aData taken at RT in CDCl_3 , except for **phos-1.1**, whose data are in CD_2Cl_2 . Values in ppm. ^bL is the isocyanide ligand used in this work.

complexes. This downfield shift can be ascribed to deshielding by the silver ion coordinated to the adjacent nitrogens, which increases with the number of metals linked to adjacent nitrogens. This shift has also been observed in other metallophosphazenes in which silver atoms are coordinated to the backbone nitrogen atoms.^{18b,c,20} The signal observed at RT is a single peak even for **phos-1.1** and **phos-1.2**, for which an AB_2 spin system corresponding to two types of phosphorus atoms would be expected. This is attributable to a fluxional process, which is typical in the coordination chemistry of silver and can be attributed to exchange phenomena involving all the phosphazene nitrogen atoms. Fluxionality can be quenched at low temperature. Thus, the single broad peak observed for the phosphazene phosphorus atoms in **phos-1.1** and **phos-1.2** at

RT is split into two signals at -80°C (as shown in Figure 1 for **phos-1.1**; see also Table 1). The signals for all compounds (either at RT or low T) appear at similar positions to those observed for the complexes $[\text{N}_3\text{P}_3(\text{NHCy})_6\{\text{AgPPh}_3\}_n](\text{TfO})_n$ ($n = 2$ or 3) mentioned before, which are also collected in Table 1 for comparison.²⁰

The ^1H NMR spectra for complexes with **phos-1** show the signals due to the isocyanide ligands and the signals corresponding to cyclohexylamino side units, which are all shifted from those in the starting complexes. In the case of the isocyanide ligands, the signals are only slightly shifted (see Experimental Section and Table 2). These signals, specifically those of NH and $\text{NH}-\text{CH}$, were verified by two-dimensional heteronuclear $^1\text{H}-^{13}\text{C}$ HSQC correlations. Most significantly,

the ^1H NMR spectra of **phos-1.1**, **phos-1.2** and **phos-1.3** all show a unique type of cyclohexylamino units at RT, as a result of the above-mentioned fluxional process. As can be observed in Table 2, coordination at phosphazene leads in all complexes to a deshielding of the protons NH, with a rise in the number of metals coordinated to adjacent nitrogens, as was also observed in the aforementioned similar silver phosphazenes, $[\text{N}_3\text{P}_3(\text{NHCy})_6\{\text{AgL}\}_n](\text{TfO})_n$ ($n = 2$ or 3 ; $L = \text{PPh}_3$ or PPh_2Me).²⁰

The signals observed for complexes with mixed-substituent trimer **phos-2** in their $^{31}\text{P}\{^1\text{H}\}$ NMR spectra at RT also shift downfield relative to the parent phosphazene (see Table 3)

Table 3. $^{31}\text{P}\{^1\text{H}\}$ NMR Spectroscopic Data for Silver Complexes with **phos-2**^a

compound	$\delta[\text{N-P-N}]$ [$^2J_{\text{P-P}}$] ^b
phos-2	20.96; 20.70 [44.3]
phos-2.1	21.20 (br, 2P), 20.6 (br, 1P)
phos-2.2	22.84 (br, 2P), 21.20 (br, 1P)
phos-2.3	23.45 ("d", 2P), 22.59 ("t", 1P) [33.0]

^aData recorded at RT in CDCl_3 except for **phos-2.2**, whose data are in CD_2Cl_2 . Values in ppm. ^bValues in Hz.

and appear at similar positions to those observed for complexes *nongem-trans*- $[\text{N}_3\text{P}_3(\text{NHCy})_3(\text{NMe}_2)_3\{\text{AgL}\}_n](\text{TfO})_n$ ($n = 2$ and 3 ; $L = \text{PPh}_3$ or PPh_2Me).²⁰ In all compounds, even in **phos-2.3** (with three silver atoms), several signals are observed because of the nongeminal-trans configuration of starting phosphazene **phos-2**.²⁴ Thus, the $^{31}\text{P}\{^1\text{H}\}$ NMR spectrum of **phos-2.3** at RT shows a single set of resonances of an AB_2 spin system, with peaks centered at $\delta = 23.45$ ("d", 2P) and 22.59 ("t", 1P), $^2J_{\text{P-P}} = 33.0$ Hz (see Figure 2, in which the $^{31}\text{P}\{^1\text{H}\}$ NMR spectra at RT of **phos-2.3** and its starting phosphazene, **phos-2**, are collected).

For **phos-2.1** and **phos-2.2**, the signals corresponding to the phosphazene phosphorus are broad as a consequence of the aforementioned fluxional process. For **phos-2.2**, two diastereomers **A** and **B** are expected (see Chart 4), namely, a pair of $R_{\text{P}2}, R_{\text{P}3}$ - or $S_{\text{P}2}, S_{\text{P}3}$ -configured enantiomers (**B**) and the diastereomer $R_{\text{P}1}, R_{\text{P}2}, S_{\text{P}3}$ - (**A**).²⁰ At -70 °C, when the fluxional process is quenched, only a single set of resonances of an AB_2 spin system is observed (at $\delta = 25.20$ ("t", 1P) and 20.41 ("d",

2P), $^2J_{\text{A-B}} = 30.1$ Hz) (see Figure 3), which seems to indicate that only one of the two stereoisomers, **A** or **B**, is present in solution. For **phos-2.1**, two diastereomers **A'** and **B'** are also expected (see Chart 5), namely, a pair of $R_{\text{P}2}, R_{\text{P}1}$ - or $S_{\text{P}2}, S_{\text{P}1}$ -configured enantiomers (**B'**) and the diastereomer $S_{\text{P}1}, S_{\text{P}2}, R_{\text{P}3}$ - (**A'**). At -60 °C, when the fluxional process is quenched, two much more complicated signals are observed (the first is centered at approximately $\delta = 22$ (m, 2P) and the second at $\delta = 19.30$ (m, 1P)), which seems to indicate that both stereoisomers **A'** and **B'** are present in solution. The spectra of both compounds remains exactly the same at -80 °C. This spectrum for **phos-2.1** is shown in the Supporting Information.

The ^1H NMR spectroscopic data of **phos-2.1**, **phos-2.2**, and **phos-2.3** are collected in Table 4. As observed for complexes with **phos-1**, coordination at phosphazene leads to a deshielding of the protons NH in all complexes. All these data are also collected in the Experimental Section, as are the $^{13}\text{C}\{^1\text{H}\}$ NMR, the mass spectral and microanalytical data for all new complexes. The assignment of the signals in the $^{13}\text{C}\{^1\text{H}\}$ NMR spectra was inferred using APT and 2D correlation HSQC and HMBC ^1H - ^{13}C spectra. The molecular cation is only observed in the mass spectra for **phos-2.1**. For the rest of compounds, peaks derived from the molecular cations are observed. In general, peaks derived from the loss of isocyanide ligands are observed.

2.2. Thermal and Mesomorphic Properties. The thermal and mesomorphic properties of silver complexes were studied by differential scanning calorimetry (DSC) and optical microscopy, and data are collected in Table 5. DSC scans for all compounds are given in the Supporting Information. It is well-known that the combination of adequate metal–ligand and flexible chains in the design of metal–lomesogens can provide complexes with a structure which is difficult to approach, or simply unapproachable, for conventional liquid crystals based on organic compounds. The cyclotriphosphazene core introduces an additional complexity to the design of liquid crystals, in particular when bulky groups are linked to the P atoms of the phosphazene ring. As a metal–ligand tecton to be linked to N atoms of this ring, the precursor $[\text{Ag}(\text{OTf})\text{L}]$ ($L = \text{CNC}_6\text{H}_4\{\text{OC}(\text{O})\text{C}_6\text{H}_2(3,4,5\text{-}(\text{OC}_{10}\text{H}_{21})_3)\}$ -4) was used. The polycatenar nature of this ligand favors the appearance of mesomorphism in the

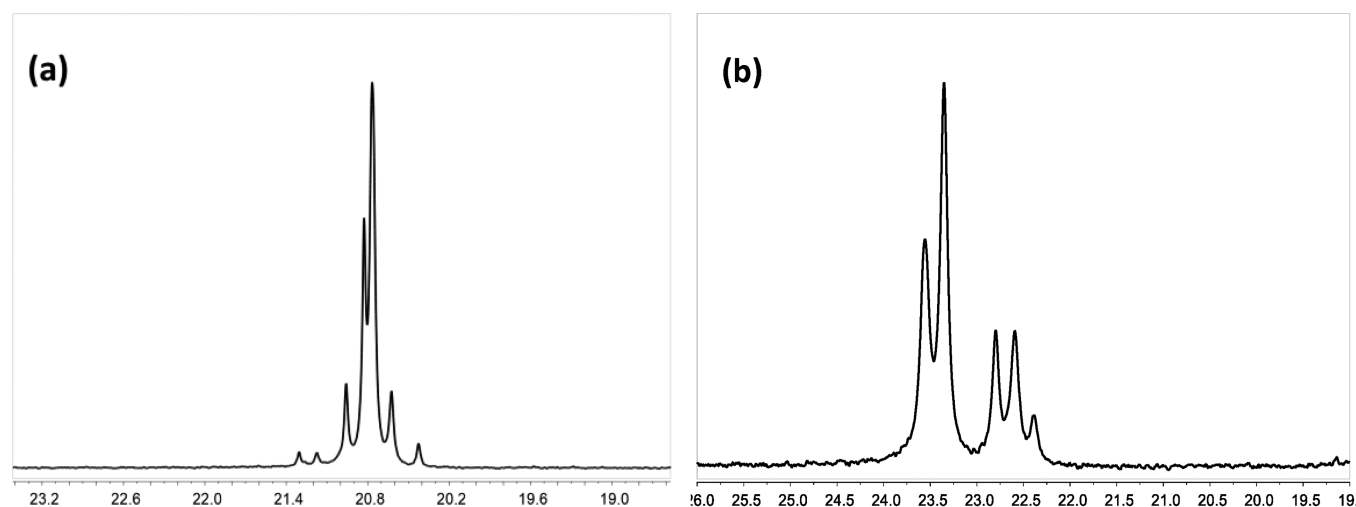


Figure 2. $^{31}\text{P}\{^1\text{H}\}$ NMR spectra at RT of (a) **phos-2** and (b) **phos-2.3** in CDCl_3 .

Chart 4. Diastereomers Expected for phos-2.2

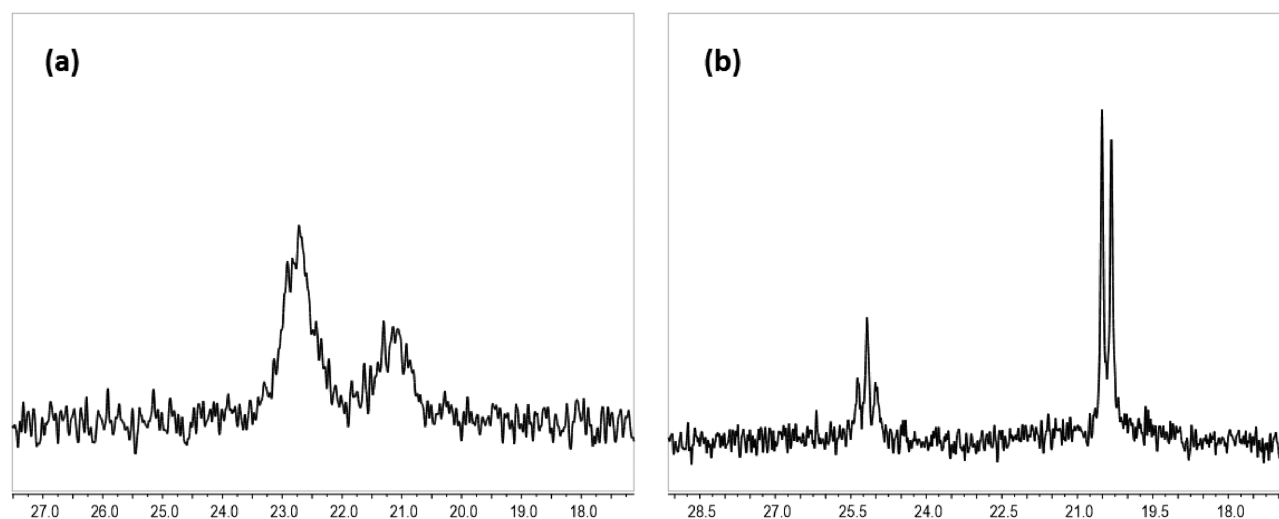
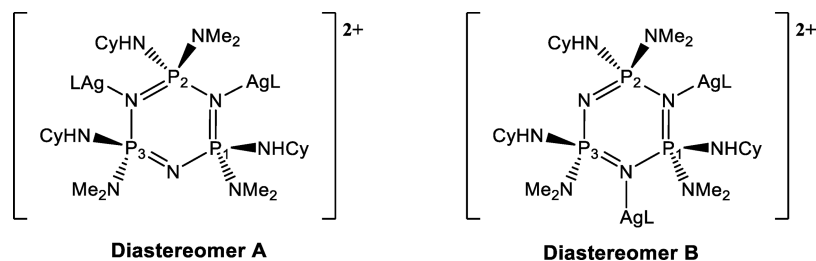
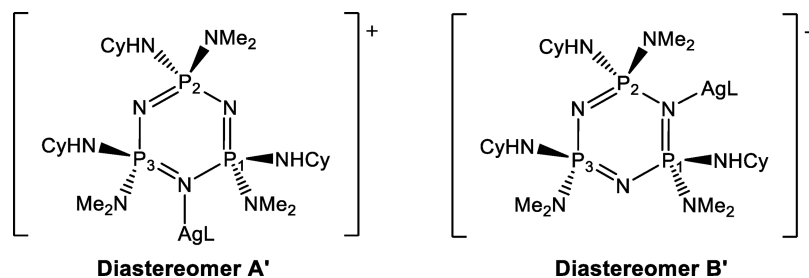
Figure 3. $^{31}\text{P}\{^1\text{H}\}$ NMR spectra of **phos-2.2** (a) at RT and (b) at $-80\text{ }^\circ\text{C}$ in CD_2Cl_2 .

Chart 5. Diastereomers Expected for phos-2.1



precursor complex $[\text{Ag}(\text{OTf})\text{L}]$. When this compound was studied under the optical microscope, a mesophase was clearly observed slightly above RT and exhibited clear evidence of thermal decomposition together with isotropization of the sample at around $145\text{ }^\circ\text{C}$. The first DSC scan of this compound exhibited an endotherm corresponding to melting transition at $33\text{ }^\circ\text{C}$ but isotropization was not clearly observed due to the thermal decomposition. Figure 4 displays the mesophase texture of a sample of this precursor that was directly heated to $145\text{ }^\circ\text{C}$ to provoke isotropization and quickly cooled below $100\text{ }^\circ\text{C}$ to minimize decomposition. Under these experimental conditions a focal conic texture with homeotropic regions was observed, which can be assigned to a hexagonal columnar mesophase (see below).

The complexation of the precursor to the cyclophosphazene ring strongly modifies the geometry of the overall molecule. The amino groups linked to the P atoms of the cyclic core hinder the efficient arrangement of these polycatenar compounds. Accordingly, the metallophosphazenes with one or two silver atoms were amorphous materials except in the

case of **phos-1.1**. On the first heating DSC scan, this compound exhibits an endotherm associated with melting followed by decomposition. The related cyclotriphosphazene with two silver units, **phos-1.2**, only exhibits a glass transition at $16\text{ }^\circ\text{C}$ before decomposition above approximately $60\text{--}70\text{ }^\circ\text{C}$. Similar cyclotriphosphazenes, **phos-2.1** and **phos-2.2**, are amorphous materials in both cases with T_g values of 15 and $18\text{ }^\circ\text{C}$, respectively. Furthermore, these compounds exhibited a higher thermal stability, and no decomposition was observed up to $100\text{ }^\circ\text{C}$. None of the cyclotriphosphazenes having either one or two silver atoms exhibited mesomorphism.

The metallophosphazenes having three silver atoms, **phos-1.3** and **phos-2.3**, are highly viscous pastes at RT. In contrast to the analogous cyclophosphazenes having one or two silver atoms, these compounds exhibited birefringent textures under the polarizing optical microscope as shown in Figure 5. In the first heating scan, the exhibited textures are poorly defined; however after shearing, a marbled-like texture was observed in accordance with a mesomorphic behavior.

Table 4. ¹H NMR Spectroscopic Data for Silver Complexes with phos-1 at Room Temperature^a

compound	$\delta(\text{CNC}_6\text{H}_4\text{O})$	$\delta[\text{C}_6\text{H}_5]$	$\delta(\text{OCH}_2)$	$\delta(\text{NH})$	$\delta(\text{N-CH})$	$\delta(\text{NMe}_2)$	$\delta(\text{CH}_2)$	$\delta(\text{CH}_3)$
L ^b	7.45 ("d", 8.9 Hz, 2H); 7.24 ("d", 8.9 Hz, 2H)	7.37 (s, 2H)	4.06 ("t", 6.6 Hz, 2H); 4.03 ("t", 6.6 Hz, 4H)				1.86–1.20 (m, 48 H)	0.88 (m, 9H)
[Ag(OTf)L]	7.63 ("d", 8.9 Hz, 2H); 7.36 ("d", 8.9 Hz, 2H)	7.37 (s, 2H)	4.07 ("t", 6.4 Hz, 4H); 4.04 ("t", 6.6 Hz, 2H)				1.86–1.23 (m, 48 H)	0.88 (m, 9H)
phos-2				1.96 (br, 3H)	3.01 (br, 3H)	2.62 (m, 18H, N = 13.6 Hz)	1.96, 1.64, 1.52, 1.26, 1.09 (m, 30H)	
phos-2.1	7.65 ("d", 8.8 Hz, 2H); 7.30 ("d", 8.8 Hz, 2H)	7.36 (s, 2H)	4.06 ("t", 6.4 Hz, 2H); 4.03 ("t", 6.4 Hz, 4H)	2.0 (br, 3H)	2.98 (br, 3H)	2.67 (m, 12H, N = 12 Hz); 2.65 (m, 6H, N = 12.4 Hz)	1.98–1.20 (m, 78H)	0.87 (m, 9H)
phos-2.2	7.71 ("d", 8.9 Hz, 4H); 7.38 ("d", 8.9 Hz, 4H)	7.38 (s, 4H)	4.05 ("t", 6.4 Hz, 4H); 4.04 ("t", 6.4 Hz, 8H)	3.78 (br, 3H)	2.99 (br, 3H)	2.77 (m, 18H, N = 14.4 Hz)	2.05–1.20 (m, 126H)	0.88 (m, 18H)
phos-2.3	7.69 ("d", 8.8 Hz, 6H); 7.35 ("d", 8.8 Hz, 6H)	7.37 (s, 6H)	4.07 ("t", 6.4 Hz, 6H); 4.04 ("t", 6.4 Hz, 12H)	4.41 (br, 1H); 4.29 (br, 2H)	3.05 (br, 3 H)	2.84 (m, 18H, N = 11.2 Hz)	2.06–1.20 (m, 174H)	0.88 (m, 27H)

^aData taken at RT in CDCl₃, except for phos-2.2, whose data are in CD₂Cl₂. Values in ppm. ^bL is the isocyanide ligand used in this work.

When compound **phos-1.3** was heated above 70 °C, a progressive isotropization was detected, which seems to be associated with a decomposition of the sample as the subsequent cooling did not lead to the appearance of the mesophase. In the first heating DSC scan of this compound (previously cooled from RT to –20 °C), a glass transition was detected at 16 °C followed by a broad endotherm at around 45 °C, immediately followed by the isotropization peak (according to the microscope observation) the broadness of which can be due to the progressive thermal decomposition. The peak at around 45 °C might be due to the melting of some residual crystalline regions (i.e., the compound is semicrystalline as obtained) since a mesophase–mesophase transition was not observed by optical microscopy. Neither isotropic–mesomorphic nor crystallization transitions were detected on the cooling process, and only a glass transition at 13 °C was detected on subsequent second heating. According to the microscopy observations, this behavior can be due to thermal decomposition when the sample was cooled down from the isotropic phase at a relatively low cooling rate.

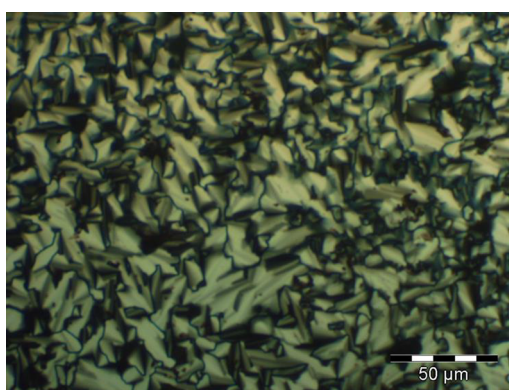
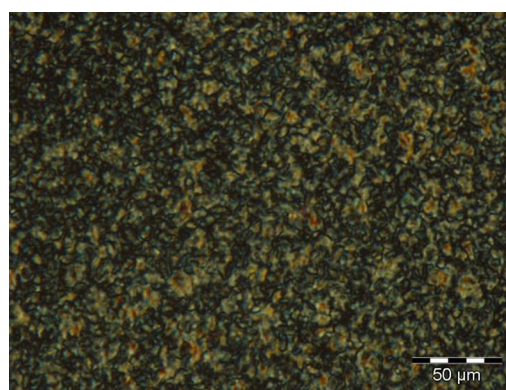
However, when **phos-2.3** was studied by optical microscopy, the isotropization was observed at a lower temperature range, around 60 °C without evidence of thermal decomposition. In this case, the subsequent cooling resulted in the appearance of a grainy texture associated with a mesophase. When the sample was annealed at around 55 °C for 1 h, close to the isotropization temperature, a blurred Schlieren-type was observed with homeotropic regions (Figure 6). If the sample is progressively cooled below RT, then the sample vitrifies maintaining this texture. This texture cannot be assigned unambiguously to a calamitic or columnar mesophase. When this compound was studied by DSC, the corresponding heating and cooling curves were essentially similar on the different scans. Thus, in the first scan a glass transition was observed at 15 °C. An endothermic peak was also observed at 61 °C corresponding to the isotropization transition in accordance with optical microscopy. On cooling, the isotropic–mesophase transition was detected at 52 °C (minimum of the peak) as an exothermic peak, with an enthalpic content similar to the corresponding isotropization transition detected on heating and followed by a vitrification process. The second heating scan was similar to the first one as is collected in Table 5. No decomposition was detected on the DSC scans even by heating the sample up to 100 °C, which seems to confirm the higher stability of series **phos-2** of these silver(I) cyclophosphazene complexes. Figure 7 exhibits the heating and cooling DSC scans of this compound (a sample was heated up to 100 °C, far from the isotropization transition, to check if decomposition takes place).

2.3. Powder X-ray Diffraction Study of the Mesophases. The structures of the liquid crystal phases of precursor [Ag(OTf)L] and derived mesomorphic compounds **phos-1.3** and **phos-2.3** were investigated by powder X-ray diffraction. X-ray diffractograms for all these compounds are given in the Supporting Information. The study of [Ag(OTf)-L] was performed at RT after heating up to 100 °C to get the mesomorphic state. When cooling down to RT, the mesophase was retained, and no crystallization was observed. The X-ray patterns recorded under these conditions were unambiguously characteristic of a hexagonal columnar mesophase. A set of five sharp spots were detected in the small-angle region with a reciprocal spacing ratio 1: $\sqrt{3}$: 2: $\sqrt{7}$: $\sqrt{12}$ (see Table 5). The five maxima correspond, respectively, to the (1 0), (1 1),

Table 5. Thermal and Mesomorphic Properties and Structural Parameters of the Synthesized Metallocyclotriphosphazenes and Silver(I) Precursor

compound	thermal transitions ^a	structural parameters ^b
[Ag(OTf)L]	1st h: K 33 (22.6) Col _h 145 I (dec) ^c	$a = 42.2$ ($d_{\text{obs}} = 36.5, 21.1, 18.0, 13.9, 10.7$)
phos-1.1	1st h: K 40 I ^d	
phos-1.2	1st h: g 16 I ^d	
phos-1.3	1st h: g 16 Col _h ^e 72 I ^d	$a = 50.7$ ($d_{\text{obs}} = 44.0, 22.0, 12.6$)
phos-2.1	1st h/2nd h: g 15 I	
phos-2.2	1st h/2nd h: g 18 I	
phos-2.3	1st h: g 15 Col _h 61 (3.6) I 2nd h: g 17 Col _h 61 (3.2) I	$a = 50.1$ ($d_{\text{obs}} = 43.5, 21.7, 14.4$)

^aData corresponding to the first (1st h) and second heating DSC scans (2nd h); scan rate: 10 °C/min. K: crystalline phase; Col_h: hexagonal columnar mesophase; I: isotropic liquid phase. Temperature in °C. The phase transition enthalpy is given in parentheses (kJ/mol). ^b a is the lattice constant of the hexagonal columnar mesophase, in Å. d_{obs} , in Å, are observed spacings. ^cDecomposition of the sample is observed. The isotropization temperature corresponds to the observation under the optical microscope. ^dDecomposition is observed at temperatures above 60–70 °C and the subsequent heating scans are not clearly reproducible due to decomposition. ^eA broad endotherm is observed at 44 °C (see text).

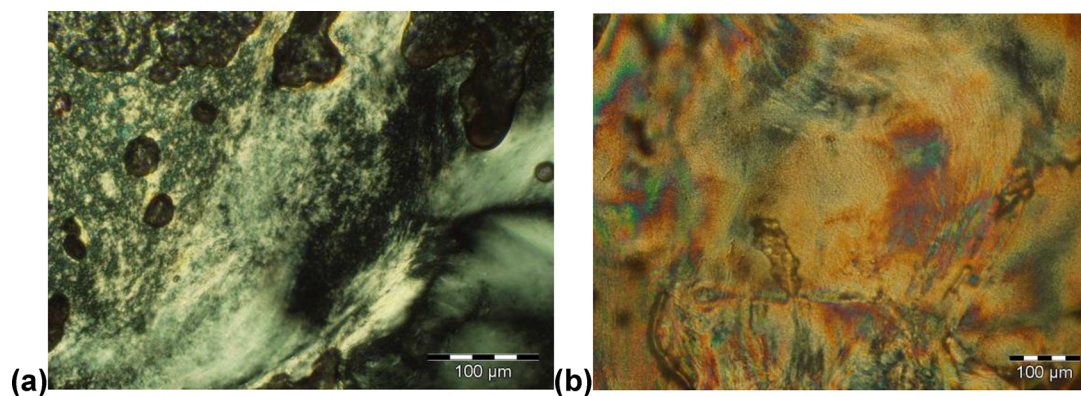
**Figure 4.** Mesomorphic texture exhibited by the precursor [Ag(OTf)L] at 80 °C.**Figure 6.** Texture exhibited by a sample of **phos-2.3** annealed at 55 °C on cooling for 1 h.

(2 0), (2 1), and (2 2) reflections of the two-dimensional hexagonal lattice and, from the measured spacings, a hexagonal lattice constant $a = 42.2$ Å can be deduced. In addition, a broad, diffuse scattering halo was detected at high angles, characteristic of the liquidlike order of the aliphatic chains, which confirms the mesomorphic nature of the phase.

For the study of complexes **phos-1.3** and **phos-2.3**, several X-ray patterns were recorded on samples of each compound at RT above glass transition, both before and after thermal treatment. The treatment consisted of fast heating of the samples to the isotropic liquid and a fast cooling to RT. Under

these conditions, the mesophase is retained, and no decomposition or crystallization phenomena are detected.

The patterns of compound **phos-1.3** are very similar under the two sets of conditions (before and after thermal treatment) and consist of three reflections at low angles corresponding to spacings of 44.0, 22.0, and 12.6 Å (see Table 5), and a broad diffuse scattering maximum at high angles corresponding to a mean distance of 4.5 Å. The three low-angle maxima are in the reciprocal ratio 1:2:√12, and this is consistent with a hexagonal packing of columns. The three maxima correspond, respectively, to the (1 0), (2 0), and (2 2) reflections of the

**Figure 5.** Texture exhibited by a sample of (a) **phos-1.3** and (b) **phos-2.3** at around 30 °C in the first heating. In the case of **phos-2.3**, the sample was previously sheared.

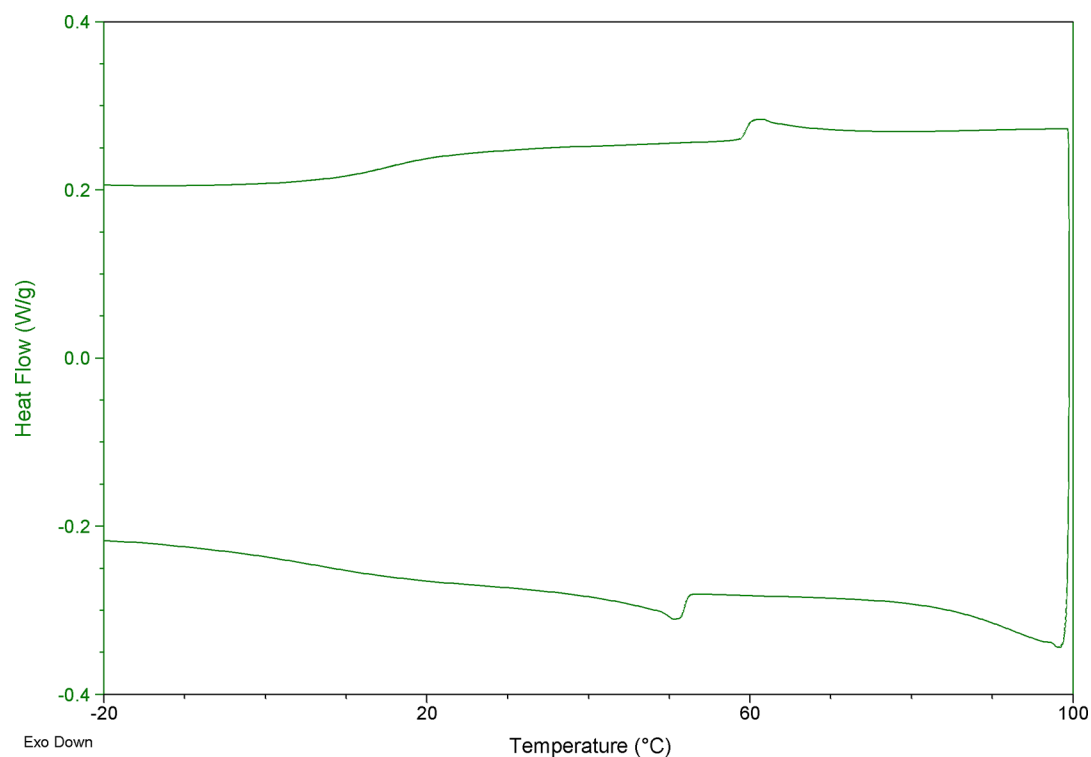


Figure 7. DSC second heating (top) and cooling (down) scans at 10 °C/min of **phos-2.3** (the sample was heated up to 100 °C to check decomposition). The baseline jump corresponds to glass transition, and the reversible mesophase-isotropic liquid transition is detected as endothermic/exothermic peaks on the heating/cooling scans.

two-dimensional hexagonal lattice, and from the measured spacings, it is deduced that the hexagonal lattice constant a is 50.7 Å. From this value, the calculated spacing for the observed reflections is 43.9, 22.0, and 12.7 Å, respectively, which is in reasonable accordance with the experimentally measured spacings. The diffuse character of the X-ray scattering observed at high angles denotes both the conformational disorder of the hydrocarbon chains in the isocyanide ligand and the absence of a fixed stacking distance of the molecules along the column axis.

Compound **phos-2.3** yields X-ray diffraction images qualitatively similar to those of **phos-1.3**. Analogous to **phos-1.3**, the patterns recorded before and after thermal treatment are practically identical: They contain a set of reflections at low angles and a broad, diffuse band at high angles corresponding to an average distance of 4.5 Å. The three low-angle maxima reflections correspond to spacings 43.5, 21.7, and 14.4 Å (see Table 5). These spacings can be indexed as the (1 0), (2 0), and (3 0) reflections of a two-dimensional hexagonal lattice with a constant a of 50.1 Å. From this value, the calculated spacing for the observed reflections is 43.4, 21.7, and 14.5 Å, respectively, which is in fair agreement with the experimentally measured spacings. The diffuse character of the high-angle X-ray scattering is characteristic of the intracolumnar disorder and is consistent with the mesomorphic nature of the columnar array.

Although the absence of a fixed stacking distance in the mesophases of these two compounds hinders the investigation of certain structural details, some calculations can be carried out to reach a rough view of the intracolumnar arrangement of the molecules. The mean intermolecular distance h along the column axis is related to the density ρ by the following equation:²⁵

$$\rho = M \times Z \times 10^{24} / (S \times h \times N_A)$$

where M is the molar mass in g, Z is the number of molecules per unit cell, S is the cross-section area of the 2D hexagonal lattice in Å² ($S = a^2 \times \sqrt{3}/2$, where a is the hexagonal lattice constant), and N_A is Avogadro's number. Using the above-mentioned formula, h can be expressed as a function of ρ and, thus, it is deduced that $h = 2.7 \times Z/\rho$ for **phos-1.3** and $h = 2.6 \times Z/\rho$ for **phos-2.3**. Considering that the density of these compounds must be close to 1 g cm⁻³,^{25,26} reasonable values for h are found when $Z = 2$. This means that two molecules of **phos-1.3** or **phos-2.3** are necessary to fill the column cross-section, and the estimated mean stacking distances $h = 5.4$ Å for **phos-1.3** and 5.2 Å for **phos-2.3** are reasonable considering the dimensions of these molecules. The driving force for intermolecular association in pairs is probably related to the peculiar geometry of these molecules that do not possess the conventional features to yield columnar mesomorphism, in particular a disk-shape. Indeed, in a starlike conformation the void spaces between the three arms of the star render efficient packing difficult. Moreover, the number of hydrocarbon chains at the periphery of the isocyanide ligands are probably insufficient to completely surround the rigid core in a single molecule, which is a requirement for decorrelating the columns and thus guarantees the mesomorphic nature of the columnar packing. Therefore, two molecules must associate to efficiently fill the column cross-section probably through some conformational change which allows each molecule to roughly adopt a half-disk shape (Figure 8). This is possible by rotation of the single bonds in the ester group of the peripheral ligand, as described by Lehmann for other star-shaped molecules.²⁷ The resulting aggregate has an approximate disk-shape and possesses a total number of 18 hydrocarbon chains, which

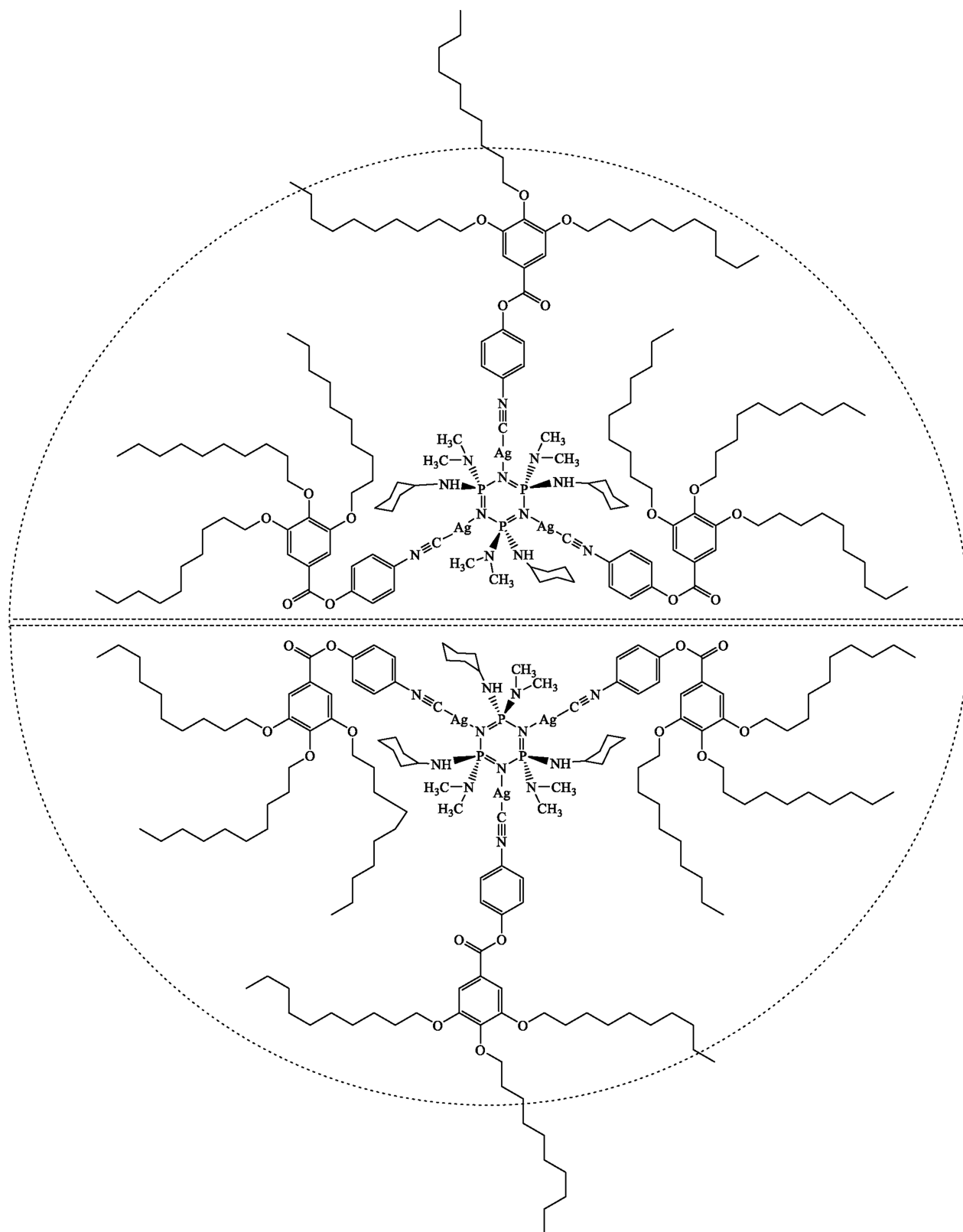


Figure 8. Folding of the starlike molecule allows adopting a half-disk-shaped conformation. Supramolecular association is driven by nanosegregation of chemically different regions and efficient space-filling. Two complementary molecules generate an overall disk shape, which promotes columnar mesomorphism.

are enough to spread out and occupy all the available space between neighboring columns. Moreover, segregation of dissimilar building blocks into different regions is achieved, and in this way, the requirements to generate columnar

mesomorphism are fulfilled. Notably, there is no evidence that the columns are generated by staking of discrete dimers. Instead, there must be a supramolecular assembling of molecules with short-range alternating orientation but with

long-range random orientation. The absence of an X-ray reflection corresponding to the repeating distance along the columnar axis supports a disordered arrangement of molecules. Due to the nonsymmetrical structure of **phos-2.3**, association in this complex can take place in different mutual orientations. However, as the liquid crystal state is fluid and dynamic, this phenomenon does not modify the shape and size of the resulting “disk”. Nevertheless, this additional degree of disorder might contribute to the differences observed in the mesomorphic properties, in particular the lower mesophase-to-isotropic liquid transition temperature of **phos-2.3** compared to that of **phos-1.3**.

Applying the above-mentioned estimation to the precursor [Ag(OTf)L], it is concluded that for a density close to 1 g cm⁻³ five molecules are needed to fill a column section of length of about 5.1 Å. The columnar structure probably consists of a central rigid core that contains the silver atoms and the triflate anions, as well as a peripheral region accommodating the conformationally disordered aliphatic chains. This model is consistent with the structures found for the columnar mesophases of similar polycatenar compounds.²⁸

3. CONCLUSIONS

The ring nitrogen atoms in the (amino)cyclotriphosphazenes [N₃P₃(NHCy)₆] (**phos-1**) and *nongem-trans*-[N₃P₃(NHCy)₃(NMe₂)₃] (**phos-2**) have shown to have sufficient basicity to coordinate to the silver(I) fragment containing a pro-mesogenic ligand, “AgL” (L = CNC₆H₄{OC(O)C₆H₂(3,4,5-(OC₁₀H₂₁)₃)}-4). Thus, the reaction of **phos-1** or **phos-2** with the silver complex [Ag(OTf)L] (L = CNC₆H₄{OC(O)C₆H₂(3,4,5-(OC₁₀H₂₁)₃)}-4; OTf = OSO₂CF₃), in different molar ratios, 1:1, 1:2, or 1:3, led to a series of two of cationic metallophosphazenes, [N₃P₃(NHCy)₆{AgL_n}(TfO)_n] (**phos-1.n**) and *nongem-trans*-[N₃P₃(NHCy)₃(NMe₂)₃{AgL_n}(TfO)_n] (**phos-2.n**) with *n* = 1, 2, or 3. According to the spectroscopic data, in all metallophosphazenes obtained, the silver fragments “AgL” are coordinated to nitrogen atoms of the phosphazene ring and the number of silver fragments (*n*) depends on the molar ratio used on the complexation. Metallocyclophosphazenes having one or two silver fragments were not liquid crystalline materials. However, **phos-1.3** and **phos-2.3**, having three silver units, were liquid crystals at RT according to the optical microscopy studies. X-ray diffraction data were in accordance with a hexagonal columnar mesophase. A model consisting of the supramolecular stacking of molecules with complementary shapes associated in pairs has been proposed to explain the columnar mesomorphism and structural parameters. The starting silver complex, [Ag(OTf)L], also exhibited a columnar hexagonal mesophase at RT.

4. EXPERIMENTAL SECTION

4.1. General Data. Infrared spectra were recorded in the range of 4000–250 cm⁻¹ on a PerkinElmer Spectrum-100 (ATR mode) FT-IR spectrometer. Carbon, hydrogen, nitrogen, and sulfur analyses were performed using a PerkinElmer 240 B microanalyser. NMR spectra were recorded on a Bruker AV 400 spectrometer. Chemical shifts are quoted relative to SiMe₄ (TMS, ¹H and ¹³C, external) and H₃PO₄ (85%) (³¹P, external) and given in parts per million (ppm). MALDI-TOF mass spectrometry was carried out on a Micromass Autospec instrument using dithranol or DCTB (trans-2-[3-(4-*tert*-butylphenyl)-2-methyl-2-propenyldiene]malononitrile) as matrix. Conductivity for compounds **phos-1.1** and **phos-1.2** was measured in dichloromethane

solution (5 × 10⁻⁴ M) with a Philips PW 9509 apparatus. DSC was performed using a DSC Q2000 from TA Instruments with samples (2–5 mg) sealed in aluminum pans and a scanning rate of 10 °C/min under a nitrogen atmosphere. In general, the peaks obtained were broad and the transition temperatures were therefore read at the maximum of the peaks. Glass transitions were read at midpoint of the baseline jump. The X-ray diffraction patterns were obtained with a pinhole camera (Anton-Paar) operating with a point-focused Ni-filtered Cu Kα beam. The samples were held in Lindemann glass capillary tubes (0.9 mm diameter) and heated, when necessary, with a variable-temperature oven. The patterns were collected on flat photographic films. The capillary axis and the film were perpendicular to the X-ray beam. Spacings were obtained using Bragg’s law.

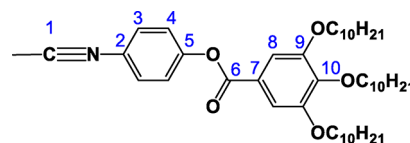
Hexachlorocyclotriphosphazene, [N₃P₃Cl₆] (Stream Chemicals), was purified by recrystallization from hot hexane and dried in vacuum. The starting cyclotriphosphazenes, [N₃P₃(NHCy)₆] and *nongem-trans*-[N₃P₃(NHCy)₃(NMe₂)₃], were prepared by a literature method.²⁰ The pro-mesogenic isocyanide was also prepared by literature method,^{4b,21a} starting from acid chlorides ClC(O)-C₆H₂(3,4,5-(OC₁₀H₂₁)₃),²⁹ which were also prepared in turn by a literature method (see the Supporting Information). Characterization data of the pro-mesogenic isocyanide are included in the text for comparison.

4.2. Synthesis and Spectroscopic Characterization Data.

4.2.1. Synthesis of [Ag(OTf)L] (L = CNC₆H₄{OC(O)C₆H₂(3,4,5-(OC₁₀H₂₁)₃)}-4). To a solution of Ag(TfO) (0.051 g, 0.2 mmol) in dry acetone (20 mL) was added isocyanide L (L = CNC₆H₄{OC(O)C₆H₂(3,4,5-(OC₁₀H₂₁)₃)}-4) (0.138 g, 0.2 mmol), and the mixture was stirred for 10 min protected from light and filtered off. Evaporation of the solvent gave the product as a white solid, which was dried in vacuo at RT for 24 h. Yield: 0.171 g (90%).

Anal. Calcd (%) for C₄₅H₆₉AgF₃N₃O₈S (948.96): C 56.96, H 7.33, N 1.48, S 3.38. Found: C 57.07, H 7.56, N 1.67, S 3.52. IR (ATR): 2197 (s) cm⁻¹ (C≡N); 1733 (s) cm⁻¹ (C=O); other bands: 1283 (m, br), 1246 (s, sh), 1222 (s), 1195 (vs), 1178 (vs), 1116 (s), 1098 (m, sh), 1027 (s) cm⁻¹. ¹H NMR ((CD₃)₂CO): δ = 7.93 (“d”, ³J_{H-H} = 8.8 Hz, 2H; CNC₆H₄O), 7.56 (“d”, ³J_{H-H} = 8.8 Hz, 2H; CNC₆H₄O), 7.45 (s, 2H; C₆H₂(OC₁₀H₂₁-p)₃), 4.10 (“t”, ³J_{H-H} = 6.4 Hz, 4H; OCH₂), 4.09 (“t”, ³J_{H-H} = 6.8 Hz, 2H; OCH₂), 1.87–1.28 (m, 48H; CH₂), 0.88 (m, 9H; CH₃). ¹H NMR (CDCl₃): δ = 7.63 (“d”, ³J_{H-H} = 8.9 Hz, 2H; CNC₆H₄O), 7.37 (s, 2H; C₆H₂(OC₁₀H₂₁-p)₃), 7.36 (“d”, ³J_{H-H} = 8.9 Hz, 2H; CNC₆H₄O), 4.07 (“t”, ³J_{H-H} = 6.4 Hz, 4H; OCH₂), 4.04 (“t”, ³J_{H-H} = 6.6 Hz, 2H; OCH₂), 1.86–1.23 (m, 48H; CH₂), 0.88 (m, 9H; CH₃). ¹⁹F NMR (CDCl₃): δ = -77.59. ¹³C{¹H} APT NMR (CDCl₃, RT) δ = CN not detected, 164.35 (1C; C₆, C(O)O); 153.30 (1C; C₅ or C₂), 153.23 (2C; C₉), 143.76 (1C; C₁₀), 128.67 (2C; C₃), 123.87 (2C; C₄), 122.83 (1C; C₇), 122.32 (1C; C₂ or C₅), 108.86 (2C; C₈), 120.58 (q, ¹J_{C-F} = 320.8 Hz, 1C; SO₂CF₃); 73.81 (1C; OCH₂), 69.50 (2C; OCH₂), 32.09, 32.06, 30.49, 29.88, 29.82, 29.77, 29.73, 29.70, 29.54, 29.49, 29.43, 26.23, 26.19, 22.85, 22.83(24C; CH₂).14.26 (3C; CH₃). MS (MALDI⁺, DCTB): *m/z* (%) = 988 (30) [M + K]⁺, 801 (100) [M - OTf + H]⁺, 1492 (40) [AgL₂]⁺.

Numbering of the C atoms of the isocyanide ligand in all complexes:



4.2.2. Synthesis of [N₃P₃(NHCy)₆]{AgL_n}(TfO)_n (phos-1.n**, *n* = 1, 2, or 3).** To a solution of [Ag(OTf)L] (0.095 g, 0.1 mmol for **phos-1.1**; 0.19 g, 0.2 mmol for **phos-1.2**; 0.285 g, 0.3 mmol for **phos-1.3**) in dry dichloromethane (15 mL) was added [N₃P₃(NHCy)₆] (72.4 mg, 0.1 mmol), and the mixture was stirred for 30 min protected from light and filtered off. The solvent was evaporated and the resulting compounds were dried in vacuo at RT for 24 h.

phos-1.1 (134 mg, yield: 80%). Elemental analysis calcd (%) for C₈₁H₁₄₁AgF₃N₁₀O₈P₃S (1672.9): C 58.16, H 8.50, N 8.37, S 1.92. Found: C 58.04, H 8.70, N 8.15, S 2.03. IR (ATR): 3313 cm⁻¹ (w,

br) (N–H); 2172 cm^{-1} (m) (C \equiv N); 1735 cm^{-1} (s) (C=O); other bands: 1289 (m), 1232 (s), 1220 (s), 1197 (vs), 1180 (s), 1118 (s), 1098 (vs), 1029 (s) cm^{-1} . $^{31}\text{P}\{^1\text{H}\}$ NMR (CDCl_3 , RT): δ = 15.60 (s, br; N_3P_3 ring). $^{31}\text{P}\{^1\text{H}\}$ NMR (CD_2Cl_2 , RT): δ = 15.19 (s, br; N_3P_3 ring). $^{31}\text{P}\{^1\text{H}\}$ NMR (CD_2Cl_2 , -80°C): δ = 15.98 (“d”, 2P), 14.09 (“t”, 1P) (AB_2 system, $^2J_{\text{P-P}} = 48.2$ Hz; N_3P_3 ring). ^1H NMR (CD_2Cl_2 , RT): δ = 7.63 (“d”, $^3J_{\text{H-H}} = 8.8$ Hz, 2H; $\text{CNC}_6\text{H}_4\text{O}$), 7.38 (s, 2H; $\text{C}_6\text{H}_2(\text{OC}_{10}\text{H}_{21}\text{-}p)_3$), 7.34 (“d”, $^3J_{\text{H-H}} = 8.8$ Hz, 2H; $\text{CNC}_6\text{H}_4\text{O}$), 4.03 (m, 6H; OCH_2), 3.0 (br, 6H, NH–CH), 2.45 (br, 6H; NH), 1.95–1.14 (m, 108H; CH_2), 0.88 (m, 9H; CH_3). ^{19}F NMR (CDCl_3 , RT): δ = -77.79 . $^{13}\text{C}\{^1\text{H}\}$ APT NMR (CDCl_3 , RT) δ = CN not detected, 164.42 (1C; C_6 , C(O)O); 153.18 (2C; C_9), 152.73 (1C; C_5 or C_2), 143.65 (1C; C_{10}), 128.58 (2C; C_3), 123.58 (2C; C_4), 122.97 (1C; C_7), 122.56 (1C; C_2 or C_3), 108.81 (2C; C_8), 120.76 (q, $^1J_{\text{C-F}} = 320.3$ Hz, 1C; SO_3CF_3), 73.76 (1C; OCH_2); 69.46 (2C; OCH_2); 50.51 (6C, NH–CH), 36.34 (12C; CH_2 , $\text{NHC}_6\text{H}_{11}$), 32.06, 32.03, 30.47, 29.85, 29.79, 29.75, 29.70, 29.68, 29.51, 29.47, 29.41, 26.20, 26.17, 25.57, 25.42, 22.80 (42C; CH_2), 14.23 (3C; CH_3). MS (MALDI $^+$, DCTB): m/z (%) = 1555.7 (90) [$\{\text{N}_3\text{P}_3(\text{NHCy})_6\}_2\text{Ag}\}^+$, 830.2 (100) [$\text{N}_3\text{P}_3(\text{NHCy})_6\text{Ag}\}^+$.

phos-1.2 (223 mg, yield: 85%). Elemental analysis calcd (%) for $\text{C}_{126}\text{H}_{210}\text{Ag}_2\text{F}_6\text{N}_{11}\text{O}_{16}\text{P}_3\text{S}_2$ (2621.86): C 57.72, H 8.07, N 5.88, S 2.45. Found: C 57.95, H 8.37, N 5.90, S 2.38. IR (ATR): 3305 cm^{-1} (m, br) (N–H); 2180 cm^{-1} (m) (C \equiv N); 1736 cm^{-1} (s) (C=O); other bands: 1280 (s), 1230 (s), 1220 (vs), 1195 (s), 1180 (vs), 1162 (s, sh), 1115 (s), 1103 (s), 1029 (s) cm^{-1} . $^{31}\text{P}\{^1\text{H}\}$ NMR (CDCl_3 , RT): δ = 16.71 (s, br; N_3P_3 ring). $^{31}\text{P}\{^1\text{H}\}$ NMR (CD_2Cl_2 , RT): δ = 16.30 (s, br; N_3P_3 ring). $^{31}\text{P}\{^1\text{H}\}$ NMR (CD_2Cl_2 , -80°C): δ = 17.18 (“t”, 1P), 13.58 (“d”, 2P) (AB_2 system, $^2J_{\text{P-P}} = 35.6$ Hz; N_3P_3 ring). ^1H NMR (CDCl_3 , RT): δ = 7.71 (“d”, $^3J_{\text{H-H}} = 8.8$ Hz, 4H; $\text{CNC}_6\text{H}_4\text{O}$), 7.37 (s, 4H; $\text{C}_6\text{H}_2(\text{OC}_{10}\text{H}_{21}\text{-}p)_3$), 7.34 (“d”, $^3J_{\text{H-H}} = 8.8$ Hz, 4H; $\text{CNC}_6\text{H}_4\text{O}$), 4.07 (“t”, $^3J_{\text{H-H}} = 6.6$ Hz, 4H; OCH_2), 4.04 (“t”, $^3J_{\text{H-H}} = 6.6$ Hz, 8H; OCH_2), 3.24 (br, 6H, NH–CH), 3.06 (br, 6H, NH), 1.96–1.13 (m, 156H; CH_2), 0.88 (m, 18H; CH_3). ^{19}F NMR (CDCl_3 , RT): δ = -77.72 (s). $^{13}\text{C}\{^1\text{H}\}$ APT NMR (CDCl_3 , RT) δ = CN not detected, 164.41 (2C; C_6 , C(O)O), 153.19 (4C; C_9), 152.83 (2C; C_5 or C_2), 143.64 (2C; C_{10}), 128.60 (4C; C_3), 123.66 (4C; C_4), 122.94 (2C; C_7), 122.37 (2C; C_2 or C_3), 108.79 (4C; C_8), 120.78 (q, $^1J_{\text{C-F}} = 321.3$ Hz, 2C; SO_3CF_3), 73.78 (2C; OCH_2); 69.45 (4C; OCH_2); 50.69 (6C, NH–CH), 36.41 (12C; CH_2 , $\text{NHC}_6\text{H}_{11}$), 32.08, 32.05, 30.48, 29.87, 29.81, 29.77, 29.72, 29.53, 29.49, 29.42, 26.22, 26.18, 25.54, 25.50, 22.83 (66C; CH_2), 14.26 (6C; CH_3). MS (MALDI $^+$, DIT): m/z (%) = 1780.3 (2) [$\text{M} - \text{L} - \text{TfO}\}^+$, 1492.2 (2) [$\text{AgL}_2\}^+$, 949.1(2) [$\text{Ag}(\text{TfO})\text{L}\}^+$, 831.7(2) [$\text{N}_3\text{P}_3(\text{NHCy})_6\text{Ag}\}^+$, 800.7 (4) [$\text{AgL}\}^+$, 724.7(100) [$\text{N}_3\text{P}_3(\text{NHCy})_6\}^+$.

phos-1.3 (339 mg, yield: 95%). Elemental analysis calcd (%) for $\text{C}_{171}\text{H}_{279}\text{Ag}_3\text{F}_9\text{N}_{12}\text{O}_{24}\text{P}_3\text{S}_3$ (3570.82): C 57.52, H 7.86, N 4.71, S 2.69. Found: C 57.30, H 7.51, N 4.53, S 2.60. IR (ATR): 3314 cm^{-1} (m, br) (N–H); 2204 cm^{-1} (m) (C \equiv N); 1737 cm^{-1} (s) (C=O); other bands: 1283 (m), 1234 (s), 1222 (vs), 1190 (s), 1176 (vs), 1162 (vs), 1112 (vs), 1091 (vs, br), 1026 (vs) cm^{-1} . $^{31}\text{P}\{^1\text{H}\}$ NMR (CDCl_3 , RT): δ = 18.97 (s; N_3P_3 ring). $^{31}\text{P}\{^1\text{H}\}$ NMR (CD_2Cl_2 , RT): δ = 18.44 (s, br; N_3P_3 ring). $^{31}\text{P}\{^1\text{H}\}$ NMR (CD_2Cl_2 , -80°C): δ = 18.35 (s; N_3P_3 ring). ^1H NMR (CDCl_3 , RT): δ = 7.71 (“d”, $^3J_{\text{H-H}} = 8.8$ Hz, 6H; $\text{CNC}_6\text{H}_4\text{O}$), 7.37 (s, 6H; $\text{C}_6\text{H}_2(\text{OC}_{10}\text{H}_{21}\text{-}p)_3$), 7.35 (“d”, $^3J_{\text{H-H}} = 8.8$ Hz, 6H; $\text{CNC}_6\text{H}_4\text{O}$), 4.07 (“t”, $^3J_{\text{H-H}} = 6.4$ Hz, 6H; OCH_2), 4.04 (“t”, $^3J_{\text{H-H}} = 6.4$ Hz, 12H; OCH_2), 3.95 (br, 6H, NH–CH), 3.08 (br, 6H, NH), 2.08–1.10 (m, 204H; CH_2), 0.88 (m, 27H; CH_3). ^{19}F NMR (CDCl_3 , RT): δ = -77.69 (s). $^{13}\text{C}\{^1\text{H}\}$ APT NMR (CDCl_3 , RT) δ = CN not detected, 164.40 (3C; C_6 , C(O)O); 153.31 (6C; C_9), 152.90 (3C; C_5 or C_2), 143.63 (3C; C_{10}), 128.93 (6C; C_3), 123.86 (6C; C_4), 122.83 (3C; C_7), 108.89 (6C; C_8); 120.05 (q, $^1J_{\text{C-F}} = 321.4$ Hz, 3C; SO_3CF_3), 73.74 (3C; OCH_2); 69.47 (6C; OCH_2); 51.47 (6C, NH–CH), 36.54, (12C; CH_2 , $\text{NHC}_6\text{H}_{11}$), 32.08, 32.05, 30.49, 29.87, 29.81, 29.77, 29.73, 29.53, 29.49, 29.42, 26.22, 26.18, 25.52, 25.2, 22.83 (90C; CH_2), 14.26 (9C; CH_3). MS (MALDI $^+$, DIT): m/z (%) = 1492.2 (1) [$\text{AgL}_2\}^+$, 949.1(1) [$\text{Ag}(\text{TfO})\text{L}\}^+$, 832.7(1) [$\text{N}_3\text{P}_3(\text{NHCy})_6\text{Ag} + \text{H}\}^+$, 800.7 (1) [$\text{AgL}\}^+$, 724.7(100) [$\text{N}_3\text{P}_3(\text{NHCy})_6\}^+$.

4.2.3. Synthesis of nongem-trans-[$\text{N}_3\text{P}_3(\text{NHCy})_3(\text{NMe}_2)_3\{\text{AgL}_n\}(\text{TfO})_n$ (phos-2.n, $n = 1, 2$, or 3). To a solution of [$\text{Ag}(\text{OTf})\text{L}$] (0.095 g, 0.1 mmol for **phos-2.1**; 0.19 g, 0.2 mmol for **phos-2.2**; 0.285 g, 0.3 mmol for **phos-2.3**) in dry dichloromethane (15 mL) was added nongem-trans- $[\text{N}_3\text{P}_3(\text{NHCy})_3(\text{NMe}_2)_3]$ (**phos-2**) (0.056 g, 0.1 mmol), and the mixture was stirred for 30 min protected from light and filtered off. The solvent was evaporated and the resulting compounds were dried in vacuo at RT for 24 h.

phos-2.1 (117 mg, yield: 77.5%). Elemental analysis calcd (%) for $\text{C}_{69}\text{H}_{123}\text{AgF}_3\text{N}_{10}\text{O}_8\text{P}_3\text{S}$ (1510.63): C 54.86, H 8.21, N 9.27, S 2.12. Found: C 54.60, H 8.44, N 9.01, S 2.10. IR (ATR): 3314 cm^{-1} (w, br) (N–H); 2182 cm^{-1} (m) (C \equiv N); 1736 cm^{-1} (s) (C=O); other bands: 1279 (m), 1247 (s), 1218 (s), 1194 (vs), 1177 (vs), 1114 (s), 1100 (s), 1028 (s) cm^{-1} . $^{31}\text{P}\{^1\text{H}\}$ NMR (CDCl_3 , RT): 21.20 (br, 2P), 20.60 (br, 1P). $^{31}\text{P}\{^1\text{H}\}$ NMR (CDCl_3 , -60°C): 22.00 (m, 2P), 19.30 (m, 1P). $^{31}\text{P}\{^1\text{H}\}$ NMR (CD_2Cl_2 , RT): 20.94 (vbr). $^{31}\text{P}\{^1\text{H}\}$ NMR (CD_2Cl_2 , -80°C): 21.93 (m, 2P), 19.41 (m, 1P). ^1H NMR (CDCl_3 , RT): δ = 7.65 (“d”, $^3J_{\text{H-H}} = 8.8$ Hz, 2H; $\text{CNC}_6\text{H}_4\text{O}$), 7.36 (s, 2H; $\text{C}_6\text{H}_2(\text{OC}_{10}\text{H}_{21}\text{-}p)_3$), 7.30 (“d”, $^3J_{\text{H-H}} = 8.8$ Hz, 2H; $\text{CNC}_6\text{H}_4\text{O}$), 4.06 (“t”, $^3J_{\text{H-H}} = 6.4$ Hz, 2H; OCH_2), 4.03 (“t”, $^3J_{\text{H-H}} = 6.4$ Hz, 4H; OCH_2), 2.98 (br, 3H, NH–CH), 2.67 (m, N = 12 Hz, 12H, NMe_2), 2.65 (m, N = 12.4 Hz, 6H, NMe_2), 2.00 (br, 3H; NH), 1.98–1.20 (m, 78H; CH_2), 0.87 (m, 9H; CH_3). ^{19}F NMR (CDCl_3 , RT): δ = -77.88 . $^{13}\text{C}\{^1\text{H}\}$ APT NMR (CDCl_3 , RT) δ = CN not detected, 164.42 (1C; C_6 , C(O)O), 153.21 (2C; C_9), 152.87 (1C; C_5 or C_2), 143.67 (1C; C_{10}), 128.71 (2C; C_3), 123.61 (2C; C_4), 123.01 (1C; C_7), 122.36 (1C; C_2 or C_3), 108.86 (2C; C_8); 120.63 (q, $^1J_{\text{C-F}} = 320.3$ Hz, 1C; SO_3CF_3), 73.79 (1C; OCH_2); 69.50 (2C; OCH_2); 50.54 (2C; NH–CH), 50.24 (1C; NH–CH), 37.50, 37.35 (6C; NMe_2), 36.17, 35.83 (6C; CH_2 , $\text{NHC}_6\text{H}_{11}$), 32.09, 32.05, 30.49, 29.87, 29.81, 29.77, 29.72, 29.70, 29.53, 29.49, 29.44, 26.22, 26.19, 25.70, 25.63, 25.56, 25.48, 22.83 (33C; CH_2), 14.25 (3C; CH_3). MS (MALDI $^+$, DCTB): m/z (%) = 1361.9 (30) [$\text{M} - \text{TfO}\}^+$, 1231.6(100) [$\{\text{N}_3\text{P}_3(\text{NHCy})_3(\text{NMe}_2)_3\}_2\text{Ag}\}^+$.

phos-2.2 (202 mg, yield: 82%). Elemental analysis calcd (%) for $\text{C}_{114}\text{H}_{192}\text{Ag}_2\text{F}_6\text{N}_{11}\text{O}_{16}\text{P}_3\text{S}_2$ (2459.59): C 55.67, H 7.87, N 6.26, S 2.61. Found: C 56.01, H 8.21, N 6.40, S 2.41. IR (ATR): 3300 cm^{-1} (m, br) (N–H); 2185 cm^{-1} (m) (C \equiv N); 1737 cm^{-1} (s) (C=O); other bands: 1282 (s), 1230 (s), 1221 (vs), 1195 (s), 1178 (vs), 1162 (s), 1114 (s), 1091 (s), 1029 (s) cm^{-1} . $^{31}\text{P}\{^1\text{H}\}$ NMR (CD_2Cl_2 , RT): δ = 22.84 (br, 2P), 21.20 (br, 1P). $^{31}\text{P}\{^1\text{H}\}$ NMR (CD_2Cl_2 , -80°C): δ = 25.20 (“t”, 1P), 20.41 (“d”, 2P) (AB_2 system, $^2J_{\text{A-B}} = 30.1$ Hz). ^1H NMR (CD_2Cl_2 , RT): δ = 7.71 (“d”, $^3J_{\text{H-H}} = 8.9$ Hz, 4H; $\text{CNC}_6\text{H}_4\text{O}$), 7.38 (s, 4H; $\text{C}_6\text{H}_2(\text{OC}_{10}\text{H}_{21}\text{-}p)_3$), 7.38 (“d”, $^3J_{\text{H-H}} = 8.9$ Hz, 4H; $\text{CNC}_6\text{H}_4\text{O}$), 4.05 (“t”, $^3J_{\text{H-H}} = 6.4$ Hz, 4H; OCH_2), 4.04 (“t”, $^3J_{\text{H-H}} = 6.4$ Hz, 8H; OCH_2), 3.78 (br, 3H; NH), 2.99 (br, 3H; NH–CH), 2.77 (m, N = 14.4 Hz, 18H; NMe_2), 2.05–1.20 (m, 126H; CH_2), 0.88 (m, 18H; CH_3). ^{19}F NMR (CD_2Cl_2 , RT): δ = -77.88 . $^{13}\text{C}\{^1\text{H}\}$ APT NMR (CDCl_3 , RT) δ = CN not detected, 164.42 (2C; C_6 , C(O)O), 153.19 (4C; C_9), 152.81 (2C; C_5 or C_2), 143.63 (2C; C_{10}), 128.68 (4C; C_3), 123.62 (4C; C_4), 122.95 (2C; C_7), 122.45 (2C; C_2 or C_3), 108.79 (4C; C_8); 120.77 (q, $^1J_{\text{C-F}} = 322.3$ Hz, 2C; SO_3CF_3), 73.78 (2C; OCH_2); 69.46 (4C; OCH_2); 50.64 (2C; NH–CH), 50.32 (1C; NH–CH), 37.50 (4C; NMe_2), 37.35 (2C; NMe_2), 36.18, 36.10, 35.77 (6C; CH_2 , $\text{NHC}_6\text{H}_{11}$), 32.08, 32.05, 30.49, 29.87, 29.81, 29.77, 29.73, 29.70, 29.53, 29.49, 29.42, 26.22, 26.19, 25.66, 25.59, 25.50, 22.85, 22.83 (57C; CH_2), 14.26 (6C; CH_3). MS (MALDI $^+$, DIT): m/z (%) = 1492.2 (1) [$\text{AgL}_2\}^+$, 800.7 (1) [$\text{AgL}\}^+$, 669.6(2) [$\text{N}_3\text{P}_3(\text{NHCy})_3(\text{NMe}_2)_3\text{Ag}\}^+$, 562.5(100) [$\text{N}_3\text{P}_3(\text{NHCy})_3(\text{NMe}_2)_3 + \text{H}\}^+$.

phos-2.3 (290 mg, yield: 85%). Elemental analysis calcd (%) for $\text{C}_{159}\text{H}_{261}\text{Ag}_3\text{F}_9\text{N}_{12}\text{O}_{24}\text{P}_3\text{S}_3$ (3408.55): C 56.03, H 7.72, N 4.93, S 2.82. Found: C 55.95, H 7.61, N 4.51, S 2.60. IR (ATR): 3292 cm^{-1} (m, br) (N–H); 2204 cm^{-1} (m) (C \equiv N); 1737 cm^{-1} (s) (C=O); other bands: 1283 (m), 1237 (s), 1221 (vs), 1187 (s), 1178 (vs), 1162 (vs), 1114 (vs), 1092 (vs, br), 1027 (vs) cm^{-1} . $^{31}\text{P}\{^1\text{H}\}$ NMR (CDCl_3 , RT): δ = 23.45 (“d”, 2P), 22.59 (“t”, 1P) (AB_2 system, $^2J_{\text{A-B}} = 33.0$ Hz). ^1H NMR (CDCl_3 , RT): δ = 7.69 (“d”, $^3J_{\text{H-H}} = 8.8$ Hz, 6H; $\text{CNC}_6\text{H}_4\text{O}$), 7.37 (s, 6H; $\text{C}_6\text{H}_2(\text{OC}_{10}\text{H}_{21}\text{-}p)_3$), 7.35 (“d”, $^3J_{\text{H-H}} = 8.8$ Hz, 6H; $\text{CNC}_6\text{H}_4\text{O}$), 4.41 (br, 1H, NH), 4.29 (br, 2H,

NH), 4.07 ("t", $^3J_{\text{H-H}} = 6.4$ Hz, 6H; OCH₂), 4.04 ("t", $^3J_{\text{H-H}} = 6.4$ Hz, 12H; OCH₂), 3.05 (br, 3H, NH-CH), 2.84 (m, N= 11.2 Hz, 18H; NMe₂), 2.06–1.20 (m, 174H; CH₂), 0.88 (m, 27H; CH₃). ¹⁹F NMR (CDCl₃, RT): $\delta = -77.72$. ¹³C{¹H} APT NMR (CDCl₃, RT) $\delta = \text{CN not detected, 164.34 (3C; C(O)O); 153.29 (3C; C}_5 \text{ or C}_2\text{), 153.21 (6C; C}_9\text{), 143.75 (3C; C}_{10}\text{), 128.80 (6C; C}_3\text{), 123.80 (6C; C}_4\text{), 122.85 (3C; C}_7\text{), 122.21 (3C; C}_2 \text{ or C}_5\text{), 108.86 (6C; C}_8\text{), 120.62 (q, } ^1J_{\text{C-F}} = 320.0 \text{ Hz, 3C; SO}_3\text{CF}_3\text{), 73.80 (3C; OCH}_2\text{), 69.44 (4C; OCH}_2\text{); 51.82 (3C; NH-CH), 37.75 (6C; NMe}_2\text{), 36.41, 35.82 (6C; CH}_2\text{, NHC}_6\text{H}_{11}\text{), 32.08, 30.49, 29.87, 29.81, 29.77, 29.72, 29.70, 29.53, 29.49, 29.43, 26.23, 26.19, 25.61, 25.54, 25.26, 22.85, 22.83 (81C; CH}_2\text{).14.25 (6C; CH}_3\text{). MS (MALDI}^+\text{, DCTB): } m/z \text{ (%) = 1491.8 (100) [AgL}_2\text{]}^+\text{, 1361.7 (20) [N}_3\text{P}_3\text{(NHCy)}_3\text{(NMe}_2\text{)}_3\text{AgL]}^+\text{, 1231.5 (10) [(N}_3\text{P}_3\text{(NHCy)}_3\text{(NMe}_2\text{)}_3\text{)}_2\text{Ag]}^+\text{, 800.3 (65) [AgL]}^+\text{.}$

ASSOCIATED CONTENT

Supporting Information

The Supporting Information is available free of charge at <https://pubs.acs.org/doi/10.1021/acs.inorgchem.0c00124>.

Synthesis and characterization details of isocyanide ligand, L; ³¹P{¹H} NMR spectrum of compound **phos-2.1** in CD₂Cl₂ at -80 °C (Figure S1); DSC scans for all compounds **phos-1.n** ($n = 1, 2, \text{ or } 3$) and **phos-2.n** ($n = 1 \text{ or } 2$) (Figures S2–S6); and X-ray diffractograms of the precursor [Ag(OTf)L] and derived mesomorphic compounds **phos-1.3** and **phos-2.3** (Figures S7–S9, respectively) (PDF)

AUTHOR INFORMATION

Corresponding Author

Josefina Jiménez – Departamento de Química Inorgánica, Facultad de Ciencias - Instituto de Síntesis Química y Catálisis Homogénea (ISQCH), Universidad de Zaragoza-CSIC, Zaragoza 50009, Spain; orcid.org/0000-0002-3444-0851; Email: jjimvil@unizar.es

Authors

José Antonio Sanz – Departamento de Química Inorgánica, Facultad de Ciencias - Instituto de Síntesis Química y Catálisis Homogénea (ISQCH), Universidad de Zaragoza-CSIC, Zaragoza 50009, Spain

José Luis Serrano – Departamento de Química Orgánica, Facultad de Ciencias - Instituto Universitario de Nanociencia de Aragón (INA), Universidad de Zaragoza, Zaragoza 50018, Spain; Departamento de Química Orgánica, Facultad de Ciencias - Instituto de Ciencia de Materiales de Aragón (ICMA), Universidad de Zaragoza-CSIC, Zaragoza 50009, Spain; orcid.org/0000-0001-9866-6633

Joaquín Barberá – Departamento de Química Orgánica, Facultad de Ciencias - Instituto de Ciencia de Materiales de Aragón (ICMA), Universidad de Zaragoza-CSIC, Zaragoza 50009, Spain; orcid.org/0000-0001-5816-7960

Luis Oriol – Departamento de Química Orgánica, Facultad de Ciencias - Instituto de Ciencia de Materiales de Aragón (ICMA), Universidad de Zaragoza-CSIC, Zaragoza 50009, Spain; orcid.org/0000-0002-0922-5615

Complete contact information is available at: <https://pubs.acs.org/doi/10.1021/acs.inorgchem.0c00124>

Notes

The authors declare no competing financial interest.

ACKNOWLEDGMENTS

This work was funded by the Ministerio de Economía y Competitividad (MINECO)-FEDER, under the project grant number MAT2017-84838P, and Gobierno de Aragón-FEDER (Liquid Crystals and Polymers Group E47_17R, FEDER 2014-2020 “Construyendo Europa desde Aragón”).

REFERENCES

- (1) Serrano, J. L. *Metallomesogens. Synthesis, Properties and Applications*; VCH Weinheim 1996.
- (2) Pucci, D. *Liq. Cryst.* **2011**, *38*, 1451–1465.
- (3) (a) Bruce, D. W. Calamitics, Cubics, and Columnar Liquid-Crystalline Complexes of Silver(I). *Acc. Chem. Res.* **2000**, *33* (12), 831–840. (b) Bruce, D. W.; Dunmur, D. A.; Lalinde, E.; Maitlis, P. M.; Styring, P. 4-Alkyloxy-4'-stilbazoles: New Heterocyclic Mesogens. *Liq. Cryst.* **1988**, *3*, 385–395.
- (4) (a) Espinet, P.; Esteruelas, M. A.; Oro, L.; Serrano, J. L.; Sola, E. *Coord. Chem. Rev.* **1992**, *117*, 215–274. (b) Donnio, B.; Guillon, D.; Bruce, D. W.; Deschenaux, R. Metallomesogens. *Comprehensive Organometallic Chemistry III: From Fundamentals to Applications* **2007**, *12*, 195–293. (c) Benouazzane, M.; Coco, S.; Espinet, P.; Martín-Alvarez, J. M.; Barberá, J. Liquid crystalline behaviour in gold(I) and silver(I) ionic isocyanide complexes: smectic and columnar mesophases. *J. Mater. Chem.* **2002**, *12*, 691–696. (d) Baena, M. J.; Coco, S.; Espinet, P. The Amide Group as Modulator of Crystalline and Liquid Crystalline Structures in Isocyanide-Alkylamide Silver(I) Complexes. *Cryst. Growth Des.* **2015**, *15*, 1611–1618. (e) Chico, R.; Domínguez, C.; Donnio, B.; Heinrich, B.; Coco, S.; Espinet, P. Isocyanide-Triphenylene Complexes of Gold, Copper, Silver and Platinum. Coordination Features and Mesomorphic Behavior. *Cryst. Growth Des.* **2016**, *16*, 6984–6991. (f) Conejo-Rodríguez, V.; Peñas-Defrutos, M. N.; Espinet, P. 4-Pyridylisocyanide gold(I) and gold(I)-plus-silver(I) luminescent and mechanochromic materials: the silver role. *Dalton Trans.* **2019**, *48*, 10412–10416.
- (5) (a) Su, P. Y. S.; Tseng, J. C. W.; Lee, K.-M.; Wang, J.-C.; Lin, I. J. B. Tetranuclear Silver(I) Clusters Showing High Ionic Conductivity in a Bicontinuous Cubic Mesophase. *Inorg. Chem.* **2014**, *53*, 5902–5910. (b) Su, P. Y. S.; Hsu, S. J.; Tseng, J. C. W.; Hsu, H.-F.; Wang, W.-J.; Lin, I. J. B. Polynuclear Silver(I) Triazole Complexes: Ion Conduction and Nanowire Formation in the Mesophase. *Chem. - Eur. J.* **2016**, *22*, 323–330.
- (6) Torres, I.; Ruiz, M.; Phan, H.; Domínguez, N.; García, J.; Nguyen, T.-Q.; Evans, H.; Resendiz, M. J.; Baruah, T.; Metta, A.; Arif, A.; Noveron, J. C. Mesomorphic Behavior in Silver(I) *N*-(4-Pyridyl) Benzamide with Aromatic π - π Stacking Counterions. *Materials* **2018**, *11*, 1666.
- (7) (a) Mark, J. E.; Allcock, H. R.; West, R. Polyphosphazenes. In *Inorganic Polymers*; Prentice Hall: Englewood Cliffs, NJ, 1992; pp 61–141. (b) Honeyman, C. H.; Manners, I.; Morrissey, C. T.; Allcock, H. R. Ambient Temperature Synthesis of Poly(dichlorophosphazene) with Molecular Weight Control. *J. Am. Chem. Soc.* **1995**, *117*, 7035–7036. For a number of references, see also (c) Allcock, H. R. The expanding field of polyphosphazene high polymers. *Dalton Trans.* **2016**, *45*, 1856–1862.
- (8) (a) Carriedo, G. A.; Fernández-Catuxo, L.; García-Alonso, F. J.; Elipe, P.; González, P. A.; Sánchez, G. J. On the synthesis of functionalized cyclic and polymeric aryloxyphosphazenes from phenols. *J. Appl. Polym. Sci.* **1996**, *59*, 1879–1885. (b) Carriedo, G. A.; Fernández-Catuxo, L.; García-Alonso, F. J.; Gómez-Elipe, P.; González, P. A. Preparation of a New Type of Phosphazene High Polymers Containing 2,2'-Dioxybiphenyl Groups. *Macromolecules* **1996**, *29*, 5320–5325. (c) Allcock, H. R. *Phosphorus-Nitrogen Compounds*; Academic Press: New York, 1972; Chapters 6 and 7. (d) Allen, C. W. Regio- and stereochemical control in substitution reactions of cyclophosphazenes. *Chem. Rev.* **1991**, *91*, 119–135. (e) De Jaeger, R.; Gleria, M. Poly(organophosphazene)s and related compounds: Synthesis, properties and applications. *Prog. Polym. Sci.* **1998**, *23*, 179–276.

(9) For a number of references, see also (a) Gleria, M., De Jaeger, R., Eds. *Applicative Aspects of Cyclophosphazenes*; Nova Science Publishers, Inc.: New York, 2004. (b) Andrianov, A. K., Ed. *Polyphosphazenes for Biomedical Applications*; John Wiley & Sons, Inc., 2009.

(10) (a) Caminade, A.-M.; Ouali, A.; Hameau, A.; Laurent, R.; Rebout, C.; Delavaux-Nicot, B.; Turrin, C.-O.; Moineau Chane-Ching, K.; Majoral, J.-P. Cyclotriphosphazene, an old compound applied to the synthesis of smart dendrimers with tailored properties. *Pure Appl. Chem.* **2016**, *88*, 919. (b) Caminade, A.-M.; Hameau, A.; Majoral, J.-P. The specific functionalization of cyclotriphosphazenes for the synthesis of smart dendrimers. *Dalton Trans.* **2016**, *45*, 1810–1822.

(11) (a) Kim, C.; Allcock, H. R. Liquid crystalline poly(organophosphazenes). *Macromolecules* **1987**, *20*, 1726–1727. (b) Singler, R. E.; Willingham, R. A.; Lenz, R. W.; Furukawa, A.; Finkelmann, H. Liquid crystalline side-chain phosphazenes. *Macromolecules* **1987**, *20*, 1727–1728. (c) Allcock, H. R.; Kim, C. Liquid crystalline phosphazenes. High polymeric and cyclic trimeric systems with aromatic azo side groups. *Macromolecules* **1989**, *22*, 2596–2602. (d) Percec, V.; Tomazos, D.; Willingham, R. A. The influence of the polymer backbone flexibility on the phase transitions of side chain liquid crystal polymers containing 6-[4-(4-methoxy- β -methylstyryl)-phenoxy]hexyl side groups. *Polym. Bull.* **1989**, *22*, 199–206. (e) Allcock, H. R.; Kim, C. Liquid crystalline phosphazenes bearing biphenyl mesogenic groups. *Macromolecules* **1990**, *23*, 3881–3887. (f) Singler, R. E.; Willingham, R. A.; Noel, C.; Friedrich, J. C.; Bosio, L.; Atkins, E. Thermotropic liquid crystalline poly(organophosphazene). *Macromolecules* **1991**, *24*, 510–516.

(12) (a) Moriya, K.; Yano, S.; Kajiwara, M. Liquid Crystalline State in Hexakis[4-(4-cyano)biphenoxy]- and Hexakis[4-(phenylazo)-phenoxy]cyclotriphosphazenes. *Chem. Lett.* **1990**, *19*, 1039–1042. (b) Moriya, K.; Suzuki, T.; Kawanishi, Y.; Masuda, T.; Mizusaki, H.; Nakagawa, S.; Ikematsu, H.; Mizuno, K.; Yano, S.; Kajiwara, M. Liquid-crystalline phase transition in organophosphazenes. *Appl. Organomet. Chem.* **1998**, *12*, 771–779. and references therein. (c) Moriya, K.; Suzuki, T.; Yano, S.; Kajiwara, M. Liquid crystalline phase transitions in cyclotriphosphazenes with different mesogenic moieties in the side chains. *Liq. Cryst.* **1995**, *19*, 711–713. (d) Moriya, K.; Kawanishi, Y.; Yano, S.; Kajiwara, M. Mesomorphic phase transition of a cyclotetraphosphazene containing Schiff base moieties: comparison with the corresponding cyclotriphosphazene. *Chem. Commun.* **2000**, 1111–1112. (e) Moriya, K.; Ikematsu, H.; Nakagawa, S.; Yano, S.; Negita, K. Dielectric Properties of Ferroelectric Liquid Crystal Hexakis(4-(4'-(s)-6-methyloctyloxy)-biphenoxy)cyclotriphosphazene. *Jpn. J. Appl. Phys.* **2001**, *40*, L340.

(13) (a) Barberá, J.; Bardaji, M.; Jiménez, J.; Laguna, A.; Martínez, M. P.; Oriol, L.; Serrano, J. L.; Zaragoza, I. Columnar Mesomorphic Organizations in Cyclotriphosphazenes. *J. Am. Chem. Soc.* **2005**, *127*, 8994–9002. (b) Barberá, J.; Jiménez, J.; Laguna, A.; Oriol, L.; Pérez, S.; Serrano, J. L. Cyclotriphosphazene as a Dendritic Core for the Preparation of Columnar Supermolecular Liquid Crystals. *Chem. Mater.* **2006**, *18*, 5437–5445. (c) Jiménez, J.; Laguna, A.; Molter, A. M.; Serrano, J. L.; Barberá, J.; Oriol, L. Supermolecular Liquid Crystals with a Six-Armed Cyclotriphosphazene Core: From Columnar to Cubic Phases. *Chem. - Eur. J.* **2011**, *17*, 1029–1039. (d) Jiménez, J.; Callizo, L.; Serrano, J. L.; Barberá, J.; Oriol, L. Mixed-Substituent Cyclophosphazenes with Calamitic and Polycatenar Mesogens. *Inorg. Chem.* **2017**, *56*, 7907–7921.

(14) (a) Levelut, A. M.; Moriya, K. Structure of the liquid crystalline state in hexakis (4-(4'-alkyloxy)biphenoxy)cyclotriphosphazenes. *Liq. Cryst.* **1996**, *20*, 119–124. (b) Moriya, K.; Suzuki, T.; Yano, S.; Miyajima, S. ³¹P and ¹³C NMR Studies of a Liquid-Crystalline Cyclotriphosphazene Derivative: Orientational Characteristics and Contrasting Shielding Anisotropies for Inorganic and Organic Moieties. *J. Phys. Chem. B* **2001**, *105*, 7920–7927.

(15) (a) Gleria, M., De Jaeger, R., Eds. *Synthesis and Characterization of Polyphosphazenes*; Nova Science Publishers, Inc.: New York, 2004. (b) Gleria, M., De Jaeger, R., Eds. *Applicative Aspects of Polyphosphazenes*; Nova Science Publishers, Inc.: New York, 2004.

(c) Gleria, M., De Jaeger, R., Eds. *Applicative Aspects of Cyclophosphazenes*; Nova Science Publishers, Inc.: New York, 2004.

(16) (a) Allcock, H. R.; Desorcie, J. L.; Riding, G. H. The organometallic chemistry of phosphazenes. *Polyhedron* **1987**, *6*, 119–157. (b) Chandrasekhar, V.; Thomas, K. R. J. Coordination and organometallic chemistry of cyclophosphazenes and polyphosphazenes. *Appl. Organomet. Chem.* **1993**, *7*, 1–31. (c) Chandrasekhar, V.; Nagendran, S. Phosphazenes as scaffolds for the construction of multi-site coordination ligands. *Chem. Soc. Rev.* **2001**, *30*, 193–203. (d) Chandrasekhar, V.; Krishnan, V. Advances in the chemistry of chlorocyclophosphazenes. *Adv. Inorg. Chem.* **2002**, *53*, 159–211. (e) Steiner, A.; Zacchini, S.; Richards, P. I. From neutral iminophosphoranes to multianionic phosphazenes. The coordination chemistry of imino-aza-P(V) ligands. *Coord. Chem. Rev.* **2002**, *227*, 193–216. (f) Pertici, P.; Vitulli, G.; Gleria, M.; Facchin, G.; Milani, R.; Bertani, R. Metal-Containing Poly(Organophosphazenes). *Macromol. Symp.* **2006**, *235*, 98–114.

(17) (a) Diefenbach, U.; Cannon, A. M.; Stromburg, B. E.; Olmeijer, D. L.; Allcock, H. R. Synthesis and metal coordination of thioether containing cyclo- and poly(organophosphazenes). *J. Appl. Polym. Sci.* **2000**, *78*, 650–661. (b) Itaya, T.; Inoue, K. Construction of hairy-rod coordination polymers with lamellar structure by self-assembling of hexakis(4-pyridylmethoxy)cyclotriphosphazene and silver alkylsulfonates. *Polyhedron* **2002**, *21*, 1573–1578. (c) Ainscough, E. W.; Brodie, A. M.; Depree, C. V.; Jameson, G. B.; Otter, C. A. Polymer Building Blocks: Self-Assembly of Silver(I) Cyclotriphosphazene Cationic Columns. *Inorg. Chem.* **2005**, *44*, 7325–7327. (d) Ainscough, E. W.; Brodie, A. M.; Davidson, R. J.; Otter, C. A. The first coordination polymer containing a chiral cyclotriphosphazene ligand. *Inorg. Chem. Commun.* **2008**, *11*, 171–174. (e) Chandrasekhar, V.; Suriya Narayanan, R. Metalation studies of 3- and 4-pyridyloxycyclophosphazenes: metallamacrocycles to coordination polymers. *Dalton Trans.* **2013**, *42*, 6619–6632. (f) Ainscough, E. W.; Brodie, A. M.; Davidson, R. J.; Jameson, G. B.; Otter, C. A. Flexible pyridyloxy-substituted cyclotetraphosphazene platforms linked by silver(I). *CrystEngComm* **2013**, *15*, 4379–4385. (g) Gutowska, N.; Seliger, P.; Andrijewski, G.; Siwy, M.; Malecka, M.; Kusz, J. Single and double crown macrocyclic derivatives of cyclotriphosphazene as receptors of silver(I) ions. *RSC Adv.* **2015**, *5*, 38435–38442. (h) Davarci, D.; Gur, R.; Besli, S.; Senkuytu, E.; Zorlu, Y. Silver(I) coordination polymers assembled from flexible cyclotriphosphazene ligand: structures, topologies and investigation of the counteranion effects. *Acta Crystallogr., Sect. B: Struct. Sci., Cryst. Eng. Mater.* **2016**, *B72*, 344–356.

(18) (a) Wisian-Neilson, P.; García-Alonso, F. J. Coordination of poly(methylphenylphosphazene) and poly(dimethylphosphazene). *Macromolecules* **1993**, *26*, 7156–7160. (b) García-Alonso, F. J.; Wisian-Neilson, P. Backbone Coordination of Poly(alkyl/arylphosphazenes). *Polym. Prepr.* **1993**, *34* (1), 264–265. (c) Chen-Yang, Y. W.; Hwang, J. J.; Kau, J. Y. Polybisaminophosphazene-Silver Nitrate Complexes: Coordination and Properties. *J. Polym. Sci., Part A: Polym. Chem.* **1997**, *35*, 1023–1031. (d) Richards, P. I.; Steiner, A. Cyclophosphazenes as Nodal Ligands in Coordination Polymers. *Inorg. Chem.* **2004**, *43*, 2810–2817. (e) Gonsior, M.; Antonijevic, S.; Krossing, I. Silver Complexes of Cyclic Hexachlorotriphosphazene. *Chem. - Eur. J.* **2006**, *12*, 1997–2008. (f) Benson, M. A.; Zacchini, S.; Boomishankar, R.; Chan, Y.; Steiner, A. Alkylation and Acylation of Cyclotriphosphazenes. *Inorg. Chem.* **2007**, *46*, 7097–7108. (g) Richards, P. I.; Bickley, J. F.; Boomishankar, R.; Steiner, A. In situ recrystallisation of a coordination polymer with hemilabile linkers. *Chem. Commun.* **2008**, 1656–1658.

(19) (a) Jiménez, J.; Laguna, A.; Benouazzane, M.; Sanz, J. A.; Díaz, C.; Valenzuela, M. L.; Jones, P. G. Metallocyclo- and Polyphosphazenes Containing Gold or Silver: Thermolytic Transformation into Nanostructured Materials. *Chem. - Eur. J.* **2009**, *15*, 13509–13520. (b) Díaz, C.; Valenzuela, M. L.; Laguna, A.; Lavayen, V.; Jiménez, J.; Power, L. A.; O'Dwyer, C. Metallophosphazene Precursor Routes to the Solid-State Deposition of Metallic and Dielectric Microstructures and Nanostructures on Si and SiO₂. *Langmuir* **2010**, *26* (12), 10223–10233.

(20) Gascón, E.; Maisanaba, S.; Otal, I.; Valero, E.; Repetto, G.; Jones, P. G.; Jiménez, J. (Amino)cyclophosphazenes as multisite ligands for the synthesis of antitumoral and antibacterial silver(I) complexes. *Inorg. Chem.* **2020**, *59*, 2464–2483.

(21) (a) Coco, S.; Espinet, P.; Martín-Alvarez, J. M.; Levelut, A.-M. Effects of isocyanide substituents on the mesogenic properties of halogeno(isocyanide)gold complexes: calamitic and discotic liquid crystals. *J. Mater. Chem.* **1997**, *7*, 19–23. (b) Jia, G.; Puddephatt, R. J.; Vittal, J. J.; Payne, N. C. Rigid-rod compounds: monomeric and oligomeric complexes with gold(I) centers bridged by (isocyanoaryl)acetylides. *Organometallics* **1993**, *12*, 263–265. (c) Jia, G.; Payne, N. C.; Vittal, J. J.; Puddephatt, R. J. (Isocyanoaryl)acetylides as Bridging Ligands in Rigid-Rod Polymers: Mononuclear and Oligonuclear Gold(I) Complexes. *Organometallics* **1993**, *12*, 4771–4778. (d) Jia, G.; Puddephatt, R. J.; Scott, J. D.; Vittal, J. J. Organometallic polymers with gold(I) centers bridged by diphosphines and diacetylides. *Organometallics* **1993**, *12*, 3565–3574.

(22) Bardaji, M.; Crespo, O.; Laguna, A.; Fischer, A. K. Structural characterization of silver (I) complexes $[\text{Ag}(\text{O}_3\text{SCF}_3)(\text{L})]$ ($\text{L} = \text{PPh}_3$, PPh_2Me , SC_4H_8) and $[\text{AgL}_n](\text{CF}_3\text{SO}_3)$ ($n = 2-4$), ($\text{L} = \text{PPh}_3$, PPh_2Me). *Inorg. Chim. Acta* **2000**, *304*, 7–16.

(23) (a) Lawrance, G. A. Coordinated Trifluoromethanesulfonate and Fluorosulfate. *Chem. Rev.* **1986**, *86*, 17–33. (b) Johnston, D. H.; Shriver, D. F. Vibrational Study of the Trifluoromethanesulfonate Anion: Unambiguous Assignment of the Asymmetric Stretching Modes. *Inorg. Chem.* **1993**, *32*, 1045–1047.

(24) In the nongeminal-2,4,6-*trans*-configuration, each substituent is linked to one phosphorous atom with two substituents towards one side about the average plane of the phosphazene ring and the third towards the other.

(25) (a) Coco, S.; Cordovilla, C.; Domínguez, C.; Donnio, B.; Espinet, P.; Guillon, D. Columnar mesophases in hybrid organic-inorganic supramolecular aggregates: Liquid crystals of Fe, Cr, Mo, and W at room temperature, built from triazines and metalloacid complexes. *Chem. Mater.* **2009**, *21*, 3282–3289. (b) Chico, R.; Domínguez, C.; Donnio, B.; Coco, S.; Espinet, P. Liquid crystalline salen manganese(III) complexes. Mesomorphic and catalytic behaviour. *Dalton Trans.* **2011**, *40*, 5977–5983. (c) Domínguez, C.; Donnio, B.; Coco, S.; Espinet, P. Supramolecular aggregates of metallo-organic acids with stilbazoles. Formation of columnar mesophases and Langmuir films. *Dalton Trans.* **2013**, *42*, 15774–15784. (d) Coelho, R. L.; Westphal, E.; Mezalira, D. Z.; Gallardo, H. Polycatenar liquid crystals based on bent-shaped chalcone and cyanopyridine molecules. *Liq. Cryst.* **2016**, *44*, 405–416. (e) Ohta, K.; Yamaguchi, N.; Yamamoto, I. Discotic liquid crystals of transition metal complexes. Part 24. Synthesis and mesomorphism of porphyrin derivatives substituted with two or four bulky groups. *J. Mater. Chem.* **1998**, *8*, 2637–2650. (f) Yoshio, M.; Konishi, R.; Sakamoto, T.; Kato, T. Bisphenylsulfone-based molecular assemblies: polar columnar liquid crystals aligned in electric fields and fibrous aggregates in organic solvents. *New J. Chem.* **2013**, *37*, 143–147.

(26) (a) Lehmann, M. Star-Shaped Mesogens – Hekates: The Most Basic Star Structure with Three Branches. In *Liquid Crystals. Materials Design and Self-assembly*; Tschierske, C., Ed.; Springer: Heidelberg, Germany, 2012; Chapter 3, p 205. (b) Lehmann, M. Star-Shaped Mesogens. In *Handbook of Liquid Crystals*; Goodby, J. W., Collings, P. J., Kato, T., Tschierske, C., Gleeson, H., Raynes, P., Vill, V., Eds.; Wiley: Weinheim, Germany, 2014; Vol. 5, Chapter 5, p 264. (c) Levelut, A.-M.; Fang, Y. Structural study of the lamellar to columnar transition in thermotropic liquid crystals: The thermotropic cubic phase of some phasidic molecules. *J. Physique Coll.* **1990**, *51* (C7), 229–236. (d) Artzner, F.; Veber, M.; Clerc, M.; Levelut, A.-M. Evidence of nematic, hexagonal and rectangular columnar phases in thermotropic ionic liquid crystals. *Liq. Cryst.* **1997**, *23*, 27–33.

(27) (a) Lehmann, M. Star mesogens (Hekates)-tailor-made molecules for programming supramolecular functionality. *Chem. - Eur. J.* **2009**, *15*, 3638–3651. (b) Detert, H.; Lehmann, M.; Meier, H. Star-shaped conjugated systems. *Materials* **2010**, *3*, 3218–3330.

(28) Benouazzane, M.; Coco, S.; Espinet, P.; Barberá, J. Supramolecular organization in copper(I) isocyanide complexes: copper(I) liquid crystals from a simple molecular structure. *J. Mater. Chem.* **2001**, *11*, 1740–1744.

(29) Furniss, B. S.; Hannaford, A. J.; Smith, P. W. G.; Tatchell, A. R. *Vogel's Textbook of Practical Organic Chemistry*; Pearson-Prentice Hall: Essex, 1989; p 692.